Sensitivity of C-Band Polarimetric Radar–Based Drop Size Estimates to Maximum Diameter

LAWRENCE D. CAREY

Department of Atmospheric Science, University of Alabama in Huntsville, Huntsville, Alabama

WALTER A. PETERSEN

NASA Goddard Space Flight Center, Wallops Flight Facility, Wallops Island, Virginia

(Manuscript received 27 March 2014, in final form 23 December 2014)

ABSTRACT

Estimating raindrop size has been a long-standing objective of polarimetric radar–based precipitation retrieval methods. The relationship between the differential reflectivity Z_{dr} and the median volume diameter D_0 is typically derived empirically using raindrop size distribution observations from a disdrometer, a raindrop physical model, and a radar scattering model. Because disdrometers are known to undersample large raindrops, the maximum drop diameter D_{max} is often an assumed parameter in the rain physical model. C-band Z_{dr} is sensitive to resonance scattering at drop diameters larger than 5 mm, which falls in the region of uncertainty for D_{max}. Prior studies have not accounted for resonance scattering at C band and D_{max} uncertainty in assessing potential errors in drop size retrievals. As such, a series of experiments are conducted that evaluate the effect of D_{max} parameterization on the retrieval error of D_0 from a fourth-order polynomial function of C-band Z_{dr} by varying the assumed D_{max} through the range of assumptions found in the literature. Normalized bias errors for estimating D_0 from C-band Z_{dr} range from −8% to 15%, depending on the postulated error in D_{max}. The absolute normalized bias error increases with C-band Z_{dr}, can reach 10% for Z_{dr} as low as 1–1.75 dB, and can increase from there to values as large as 15%–45% for larger Z_{dr}, which is a larger potential bias error than is found at S and X band. Uncertainty in D_{max} assumptions and the associated potential D_0 retrieval errors should be noted and accounted for in future C-band polarimetric radar studies.

1. Introduction

a. Background

The estimation of raindrop size distribution (DSD) parameters, including the central tendency of the DSD (mean or median drop size), has been a primary objective of polarimetric radar since the pioneering theoretical study of Seliga and Bringi (1976). Using surface disdrometer measurements of a heavy-rain event, Seliga et al. (1986) demonstrated that simulated differential reflectivity Z_{dr} could provide reasonably accurate estimates of the median volume diameter D_0 when the $D_0 = F(Z_{dr})$ relation is derived from the disdrometer DSD observations and a radar scattering model. Observational studies focused on the estimation of D_0 or the mass-weighted mean diameter D_m from radar measurements of Z_{dr} alone and found reasonably good agreement with ground-based disdrometer (Goddard et al. 1982; Goddard and Cherry 1984; Aydin et al. 1987) and airborne particle imaging probe (Bringi et al. 1998) estimates. According to these empirical radar studies, Z_{dr}-based estimates of D_0 (or D_m) have an absolute normalized bias error ≤ 5% and a normalized standard error of 7%–15% relative to disdrometer or probe measurements of D_0 (or D_m), which is consistent with the simulations of Seliga et al. (1986) and also Jameson (1994).

These early studies provide an analysis framework in which DSD parameters can be estimated directly from polarimetric radar observations using equations derived from disdrometer DSD measurements as input to a radar scattering model. Beyond DSD, the derived $D_0(Z_{dr})$ equation is dependent on other details of the rain model, including the assumed drop shape versus size relation (Goddard et al. 1982; Goddard and Cherry 1984; Bringi

Corresponding author address: Lawrence D. Carey, Dept. of Atmospheric Science, University of Alabama in Huntsville, 320 Sparkman Drive, Huntsville, AL 35805.
E-mail: larry.carey@nsstc.uah.edu

DOI: 10.1175/JAMC-D-14-0079.1

© 2015 American Meteorological Society

et al. 1998; Thurai and Bringi 2005). Drop oscillations and canting tend to bias the drop shape slightly toward a more spherical shape in a manner that is nonlinear with diameter (Chandrasekar et al. 1988; Beard et al. 1991; Bringi et al. 1998; Thurai and Bringi 2005; Thurai et al. 2009). The sensitivity of $D_0(Z_{dr})$ to uncertainty in the drop shape versus size relation led Bringi et al. (2002) and Gorgucci et al. (2002) to develop the so-called effective β method for deriving DSD parameters (D_0, N_w, μ) of an assumed gamma distribution (Ulbrich 1983) from the triplet of observed horizontal reflectivity Z_h, Z_{dr}, and specific differential phase K_{dp}. The method takes advantage of the combined use of K_{dp} and Z_{dr} to mitigate the effects of drop oscillation and canting by estimating the slope β of an assumed linear relationship between drop shape and size. The effective β method has been applied to polarimetric radar observations in a wide variety of climate regimes, and the retrieved DSD parameters were in general agreement with surface disdrometers (Bringi et al. 2002, 2003).

Brandes et al. (2004a) demonstrated that the estimation error for β due to measurement error in K_{dp} is very large for $K_{dp} < 1.5°\,\mathrm{km}^{-1}$, thereby limiting the practical utility of the effective β method for DSD retrieval to heavy rain (e.g., rain rate $R > 70\,\mathrm{mm\,h}^{-1}$ at S band or $R > 40\,\mathrm{mm\,h}^{-1}$ at C band). The retrieval of D_0 must often default to a Z_{dr}-only approach in many rainfall situations (Zhang et al. 2001; Bringi et al. 2002, 2006, 2009; Brandes et al. 2003, 2004a,b). Fortunately, significant progress has been made in the experimental measurement of drop shape over a wide range of sizes (Beard and Kubesh 1991; Andsager et al. 1999; Thurai and Bringi 2005; Thurai et al. 2007). The empirical results (e.g., Thurai and Bringi 2005; Thurai et al. 2007) are generally consistent with the range of axis ratios predicted by theory (Beard and Chuang 1987). Since there appears to be good agreement between recent empirical drop shape–size relations in the literature (Goddard et al. 1994; Thurai and Bringi 2005; Brandes et al. 2002; Thurai et al. 2007), the estimation of D_0 from Z_{dr} can likely be accomplished without significant error because of drop shape assumptions (Brandes et al. 2003, 2004a,b; Bringi et al. 2006, 2009).

b. Motivation

Another long-standing issue in polarimetric radar rainfall retrieval methods is their potential sensitivity to DSD truncation, including assumptions regarding both maximum (D_{max}) and minimum (D_{min}) diameters (Ulbrich and Atlas 1984; Ulbrich 1985, 1992). Note that all drop diameters are in terms of the equivalent spherical diameter. Truncation of the DSD at the large diameter end of the spectrum can influence the accuracy of the gamma model parameters fit to the DSD using the method of moments (Ulbrich and Atlas 1998). Developing relations between radar observables and rainfall properties, which are both calculated from integral moments of the DSD, requires assumptions regarding the limits (D_{min}, D_{max}) of those rainfall integral parameters. Bias errors in the derived radar–rainfall relations can result simply from inappropriate assumptions regarding the limits of the DSD integrals involved (Ulbrich 1985). DSD moment errors (especially for high moments) are more sensitive to the DSD uncertainty for large raindrops (Cao et al. 2008; Cao and Zhang 2009). Therefore, the uncertain range of maximum raindrop diameter (including the truncation) could affect the accuracy of DSD retrieval. Since both D_0 and Z_{dr} are calculated from high-order moments of the DSD, the development of an accurate $D_0(Z_{dr})$ relation also depends on acceptable DSD truncation assumptions, including the choice of D_{max} (Ulbrich and Atlas 1984; Ulbrich 1992). Ulbrich and Atlas (1984) concluded that the relationship between D_0 and Z_{dr} depends strongly on D_{max} only when $D_0 \geq 2.5\,\mathrm{mm}$ for an assumed gamma DSD. Since D_{max} and D_0 appear to be proportional in DSD observations, Ulbrich and Atlas (1984) demonstrated that the relationship between D_0 and Z_{dr} for a gamma DSD is relatively insensitive to changes in D_{max}/D_0 for values of $D_0 \leq 3.2\,\mathrm{mm}$ provided $D_{max}/D_0 \geq 2.5$.

However, the measured ratio of D_{max}/D_0 rarely exceeds 2.5 in typical disdrometer sample volumes. In Keenan et al. (2001), the 95th percentile of D_{max}/D_0 in 1-min DSD data was 2.4 over Darwin, Australia. In a large sample of 1-min DSDs observed by 2D video disdrometers (2DVDs) over Huntsville, Alabama, the mean D_{max}/D_0 was 2.0 and 92.5% of the data were characterized by $D_{max}/D_0 < 2.5$ (Fig. 1) when the number of drops ≥ 300 and the rain rate $\geq 1\,\mathrm{mm\,h}^{-1}$. Using similar 2DVD instruments and thresholds, a similar result (i.e., mean $D_{max}/D_m = 1.9$) was found by Gatlin et al. (2015), who analyzed an order of magnitude more 1-min DSD samples from a variety of locations around the globe in a wide variety of precipitation conditions. As noted by Ulbrich (1992), the average D_{max}/D_0, which is observed by a single disdrometer, increases with the integration time (i.e., 1.9, 2.5, and 2.9 over 1, 10, and 30 min, respectively). Assuming the longer integration periods provide DSDs that are consistent with those found within a typical radar resolution volume, natural rainfall may typically meet the $D_{max}/D_0 \geq 2.5$ criteria required by Ulbrich and Atlas (1984) for $D_0(Z_{dr})$ estimates that are relatively insensitive to D_{max} assumptions.

However, partially compensating volumetric sampling limitations of a single disdrometer with long integration periods likely mixes DSDs from a variety of

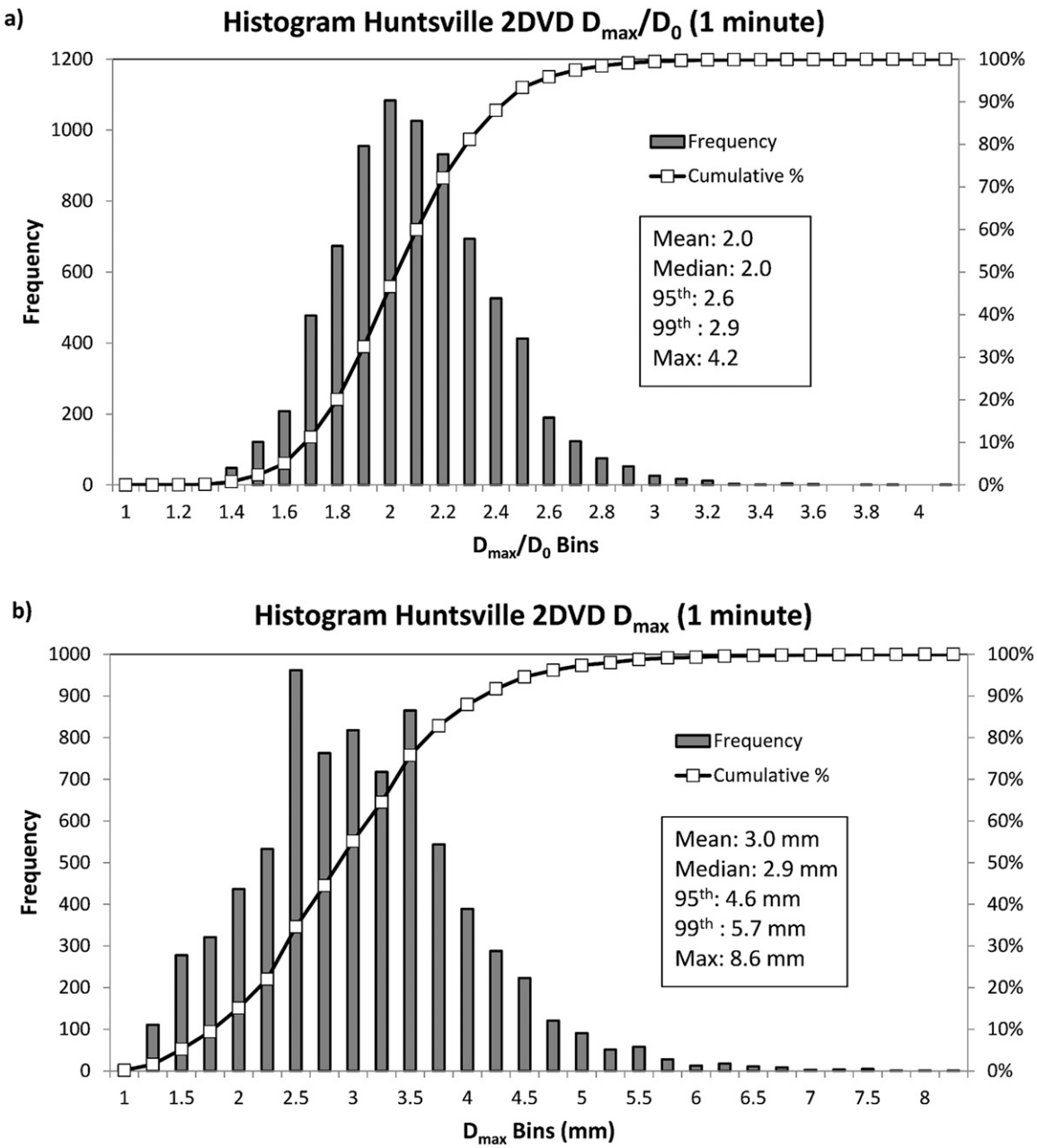

FIG. 1. Frequency histogram of (a) the ratio of the maximum diameter over the median volume diameter (D_{max}/D_0) and (b) the maximum diameter D_{max} for 7678 one-minute drop size distributions collected in a variety of rain types over Huntsville using 2DVDs. Drop size distributions were utilized when total drop concentration $N_T \geq 300$ drops, rain rate $R \geq 1.0\,\mathrm{mm\,h^{-1}}$, and no hail or other ice hydrometers were present in the sample volume. All diameters are equivalent spherical diameters.

rainfall types and microphysical processes that may not be representative of the DSDs affecting an instantaneous measurement by radar. For example, one can consider the horizontal scale of advection given various sample times. Assuming a conservative relative motion of $5\,\mathrm{m\,s^{-1}}$, a 1-km patch of rain will have moved by a disdrometer in 200 s (roughly 3 min of integration). One minute of integration results in a spatial scale of 300 m, which is about the size of a radar gate space. On the other hand, a 10–30-min integration period is equivalent to a horizontal scale of 3–9 km, which may be too large to be representative of instantaneous conditions in a radar sample. Hence, there is still some uncertainty regarding the appropriate D_{max}/D_0 in

a sample volume consistent with radar applications and hence regarding the sensitivity of $D_0(Z_{dr})$ to various D_{max} assumptions.

It is important to note that the results of Ulbrich and Atlas (1984) are specific to S band (λ = 10 cm). More recent S band studies by Brandes et al. (2003, 2004a,b) have demonstrated good agreement between polarimetric radar–based and surface disdrometer-based retrievals of DSD parameters while evaluating the constrained-gamma approach of Zhang et al. (2001). Brandes et al. (2003) suggested that their DSD parameter retrievals from S-band Z_{dr} were fairly insensitive to D_{max} assumptions. However, Brandes et al. (2003) noted that large drop regions characterized by $Z_{dr} > 3$ dB ($D_0 > 3.2$ mm) were likely not well represented by the constrained-gamma model and were therefore ignored in their studies. In that respect, Brandes et al. (2003) conclusions regarding the robustness of S-band $D_0(Z_{dr})$ retrievals are similar to Ulbrich and Atlas (1984).

Several studies have noted the impact of Mie resonance associated with large raindrops on C band (λ = 5 cm) polarimetric radar observables and rainfall retrieval algorithms (Bringi et al. 1991; Meischner et al. 1991; Aydin and Giridhar 1992; Carey et al. 2000; Zrnić et al. 2000; Keenan et al. 2001). The behavior of Z_{dr} in large (e.g., $D > 5$ mm) raindrops at C band in the Mie scattering regime is well known (e.g., Zrnić et al. 2000). Resonance occurs for drops larger than about 5 mm where C-band Z_{dr} exhibits decidedly nonmonotonic behavior, especially relative to S-band (i.e., nonresonant) Z_{dr} (Fig. 2). Deviations between C- and S-band Z_{dr} reach 3.5 dB at drop diameters just below 6 mm. By comparison, X-band Z_{dr} has a muted resonance response in raindrops larger than about 3 mm and is much closer to S-band Z_{dr}, except from 3 to 4 mm where deviations can reach up to 0.74 dB. Despite the obvious potential impact of resonance, the fundamental importance of measuring DSD central tendency, and the growing numbers of C-band polarimetric radars worldwide, no study to date has investigated the detailed sensitivity of C-band retrieval of $D_0(Z_{dr})$ to assumptions regarding D_{max}. We note that such D_{max} sensitivity studies have been conducted on the C-band polarimetric retrieval of rain rate, attenuation, and differential attenuation (Zrnić et al. 2000; Keenan et al. 2001).

In situ aircraft probe, videosonde, and surface disdrometer observations have demonstrated that large raindrops in the range of 5–8 mm, and possibly up to 9–10 mm, occur in a wide variety of rainfall regimes (Beard et al. 1986; Rauber et al. 1991; Takahashi et al. 1995; Schuur et al. 2001; Hobbs and Rangno 2004; Fujiyoshi et al. 2008; Gatlin et al. 2015). Nonetheless, large drop

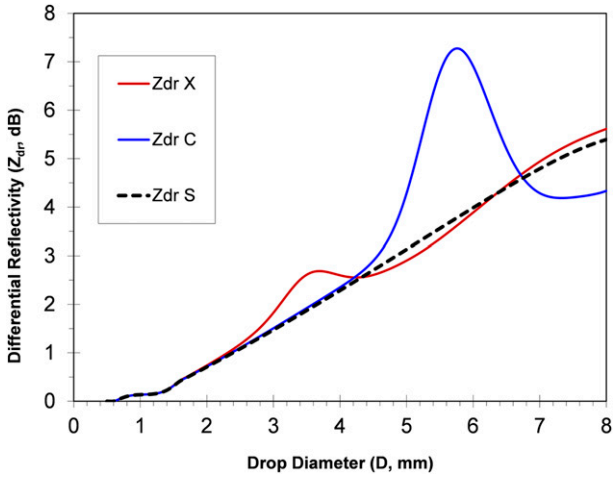

FIG. 2. The differential reflectivity (Z_{dr}; dB) of monodisperse raindrops of equivalent spherical diameter (D; mm) for X-band (red), C-band (blue), and S-band (dashed black) wavelengths. For the monodisperse simulations in this figure, the following assumptions were made: drop shape vs size relationship of Thurai et al. (2007), a drop temperature of 20°C, and a mean and standard deviation of the drop canting angle of 0° and 7.5° (Huang et al. 2008), respectively.

occurrence in disdrometer observations is rare. For example, 97% of all 1-min DSDs sampled by 2DVDs were characterized by $D_{max} < 5$ mm over Huntsville, Alabama (Fig. 1). In a 2DVD study of large ($D \geq 5$ mm) raindrop occurrence worldwide, Gatlin et al. (2015) found only 10 464 large raindrops in a total rain sample consisting of over 224 million drops (i.e., <0.004% occurrence on a per-drop basis). Because of sampling limitations, disdrometers likely undersample the number of large raindrops and hence D_{max} (Ulbrich and Atlas 1984; Ulbrich 1992; Smith et al. 1993; Keenan et al. 2001; Brandes et al. 2003). As a result, there is still considerable uncertainty regarding the appropriate D_{max} for any given rainfall situation. Reflecting this uncertainty, there is currently no consensus on the appropriate value of D_{max} to use in a C-band radar analysis framework using disdrometer observations (e.g., Zrnić et al. 2000; Keenan et al. 2001).

In C-band radar studies, parameterized values of D_{max} have been assumed to be constant in the range of 4–10 mm (Aydin and Giridhar 1992; Carey et al. 2000; Zrnić et al. 2000; Keenan et al. 2001; Tabary et al. 2009), a constant multiple C of the disdrometer observed central tendency (D_0 or D_m) where the C has ranged from 2.5 to 3.5 (e.g., $D_{max} = CD_0$) (Keenan et al. 2001; Bringi et al. 2002, 2003, 2006, 2009; Thurai et al. 2007), and the actual disdrometer-measured maximum diameter despite recognized sampling limitations (Ryzhkov and Zrnić 2005; Tabary et al. 2009). Several of these studies

have developed and applied C-band $D_0(Z_{dr})_{fit}$ best-fit relations but no sensitivity test to the D_{max} assumption has yet been conducted. As pointed out by Zrnić et al. (2000), the uncertainty in D_{max} in the range of 5–8 mm is exactly where the maximum sensitivity to resonance is expected.

Because of the sampling limitations of disdrometers, D_{max} is estimated or essentially parameterized in the studies above. In the instances where D_{max} is parameterized as a multiple of D_0 ($D_{max} = CD_0$), it is important to note that D_0 here is the disdrometer observed D_0. This approach was first taken by Keenan et al. (2001) to provide a physically realistic domain for D_{max} in the polarimetric variable scattering calculations based on the observed DSD data even though the disdrometer typically underestimates D_{max}. Multiple studies (Bringi et al. 2002, 2003, 2006, 2009; Thurai et al. 2007) have since employed Keenan et al.'s approach. To the extent that the parameterized D_{max} in the resulting rain model is different than the observed D_{max}, the resulting model D_0 will be different than the disdrometer observed D_0 even though the observed D_0 is sometimes used to parameterize D_{max} in the first place. In the studies where D_{max} is parameterized, it is the model D_0 that is used to develop the $D_0(Z_{dr})_{fit}$ equation to estimate D_0 from radar observations of Z_{dr}. More details will be provided in section 2.

c. Objectives

Because of their relative affordability, C-band polarimetric radars are in common use worldwide for both research and operations. As such, it is critical to assess errors associated with raindrop size retrievals at C band because of the uncertainty in the maximum raindrop diameter, as has been accomplished for other C-band rain algorithms such as rain rate and propagation correction (Zrnić et al. 2000; Carey et al. 2000; Keenan et al. 2001). The fundamental definition of maximum drop diameter, its impact to precipitation remote sensing algorithms, and more specific to this study, a complete characterization of potential errors in C-band radar drop size retrievals are important for a number of applications, including global physical and statistical ground validation (Chandrasekar et al. 2008) of satellite precipitation remote sensing methods such as for the NASA Global Precipitation Measurement (GPM) mission (Hou et al. 2014). Given the current uncertainty in parameterizing the large drop tail of the DSD (Zrnić et al. 2000), we conduct a D_{max} sensitivity test to assess the potential errors inherent in the development of a C-band $D_0(Z_{dr})_{fit}$ relation using disdrometer data. Because D_{max} variability is likely to have a more significant impact on D_0 retrievals at larger Z_{dr} and because of the exacerbating influence of resonance scattering at C band, errors in the retrieval of D_0 as a function of Z_{dr} are presented in addition to overall sample errors. Results at X and S band are also briefly compared with C band to highlight the important impact of resonance on these potential errors at C band. The potential effect of drop temperature is also explored.

2. Data and methodology

a. Raindrop model development

Data from the Colorado State University low-profile and NASA GPM Ground Validation compact 2DVDs (Schönhuber et al. 2008) located at the instrument berm of the National Space Science Technology Center (NSSTC) in Huntsville, Alabama, were utilized to develop an experimental raindrop model. Disdrometer data were collected in 1-min integration periods. To estimate robust DSD statistics and gamma fits to the DSD data, only 1-min periods with total drop concentration (N_T) $\geq$ 300 drops and $R \geq 1.0\,\mathrm{mm\,h^{-1}}$ were used, providing 7678 one-minute-averaged samples of the binned DSD. DSD data from the low-profile and compact 2DVD units were available from 2007 to 2011 and from late 2009 to 2011, respectively. DSD data were binned at 0.25 mm through early 2010 after which time the bin size was reduced to 0.20 mm. A comparison of results showed no significant impact of the change in bin size to the goals of this study. A comparison of the side-by-side 2DVD units by Thurai et al. (2011) demonstrated excellent agreement in measuring DSD parameters. For example, the correlation coefficient and fractional standard error between the D_m values measured by the collocated low-profile and compact 2DVDs was 0.95 and 5%, respectively.

The DSD dataset contained a wide variety of rainfall types, including convection and stratiform precipitation within ordinary thunderstorms, tropical storms, mesoscale convective systems, and severe storms occurring across all seasons of the year. One-minute-averaged DSD samples with likely hail, snow, or mixed-phase precipitation contamination were removed through manual inspection of the 2DVD fall speed data, surface temperature, available sounding data, Advanced Radar for Meteorological and Operational Research (ARMOR; Petersen et al. 2005, 2007) polarimetric observations, and NOAA *Storm Data.*

The method of truncated moments of Ulbrich and Atlas (1998) was utilized to fit a gamma distribution model (Ulbrich 1983) to the 1-min 2DVD DSD data. The method of truncated moments accounts for the finite D_{max} in the retrieval of the gamma model parameters: N_0 (intercept parameter), D_0 (median volume diameter), and μ (shape parameter). The triplet of

gamma fit parameters along with the D_{max} assumed for each sensitivity test and a constant D_{min} fully characterized the gamma rain DSD for input into the radar scattering model, which is detailed in the next paragraph. The value of D_{min} was fixed at 0.4 mm since the first bin of the 2DVD was not utilized in this study because of drop undercounting. Consistent with Ulbrich and Atlas (1998), the choice of D_{min} had little impact on the outcome of this study. The parameterized D_{max} was varied to encompass the variety of assumptions currently found in the literature, as discussed in more detail below. Note that all drop diameters (e.g., D_{min}, D_{max}, D_0) are in terms of equivalent spherical diameters. As found by Ulbrich and Atlas (1998), it is important to note that a change in DSD shape is associated with the selection of a parameterized D_{max}. In fact, that is why we derive the gamma DSD triplet of (N_0, D_0, μ) using the truncated method of moments after assuming the parameterized D_{max}. Other rain model assumptions required for input into the radar scattering model were 1) the recommended drop shape versus diameter relationship of Thurai et al. (2007), 2) a Gaussian canting angle distribution with mean of 0° and a standard deviation of 7.5° (Huang et al. 2008), and 3) a drop temperature of 20°C. The drop temperature T of T = 20°C was assumed throughout most of the study except when T = 10°C or T = 30°C was required for comparison.

b. Radar scattering model

The **T** matrix model for oblate spheroids (Waterman 1969; Barber and Yeh 1975; Bringi and Chandrasekar 2001, appendix 3, 591–594) was used to calculate the individual scattering properties of each specified raindrop diameter (and hence shape), raindrop temperature and radar wavelength. The Mueller matrix model as implemented by Vivekanandan et al. (1991) was then used to calculate the polarimetric radar observables, including Z_{dr}, for each realization of the prescribed gamma rain DSD using the specified drop canting angle and radar elevation angle. The radar elevation angle was assumed to be 0°. The radar wavelength was set to C band (5.33 cm) for the bulk of the sensitivity study except when X-band (3.17 cm) or S-band (10.7 cm) Z_{dr} was required for comparison.

c. Median volume diameter retrieval experiments

A series of experiments to estimate D_0 from Z_{dr} [i.e., $D_0(Z_{dr})_{fit}$] were conducted by varying the parameterized D_{max} through the range of assumptions found in the literature discussed in section 1, including 1) constant D_{max} = 4, 5, 6, 7, 8, 9, and 10 mm; 2) actual 2DVD-measured D_{max}; and 3) $D_{max} = CD_0$ where C = 2.0, 2.5, 3.0, 3.5, and 4.0 and D_0 here is the observed D_0 from the 2DVD observations of drop size and counts. Although likely physically unrealistic, the constant D_{max} assumptions provide a direct way to explore the impact of resonance on the behavior of $D_0(Z_{dr})_{fit}$. In the latter case of $D_{max} = CD_0$, D_{max} is capped at a maximum of 8 mm consistent with the practice of recent polarimetric studies (Bringi et al. 2006, 2009; Thurai et al. 2007) and with the idea that spontaneous raindrop breakup would typically occur around this diameter (e.g., Kamra et al. 1991). Note that constant D_{max} of 9 and 10 mm were explored to understand the sensitivity of this assumption. All other rain and radar model characteristics were fixed for calculating the intrinsic Z_{dr} associated with each DSD. To simulate the retrieval of D_0 from observed Z_{dr} in the presence of radar measurement error, Gaussian noise was added to the simulated intrinsic Z_{dr} values with a mean of 0 dB and a standard deviation of 0.25 dB. Vertically pointing scans (Gorgucci et al. 1999) can be used to mitigate bias error in Z_{dr}, thus justifying the 0 dB mean. The standard deviation of Z_{dr} is based on vertically pointing ARMOR scans of drizzle (e.g., 0.20–0.25 dB).

For each experiment, a $(D_{max})_{fit}$ was assumed to develop a fourth-order polynomial fit to estimate D_0 (mm) from Z_{dr} (dB) of the form

$$D_0(Z_{dr})_{fit} = aZ_{dr}^4 + bZ_{dr}^3 + cZ_{dr}^2 + dZ_{dr} + e, \quad (1)$$

where a, b, c, d, and e are constants derived from the Levenberg–Marquardt algorithm (Levenberg 1944; Marquardt 1963) for nonlinear least squares curve fitting. It is important to point out that the D_0 used to regress Eq. (1) comes from the gamma DSD triplet of parameters (N_0, D_0, μ) derived from the truncated method of moments using the parameterized D_{max} assumptions described above. The choice of a high-order polynomial for Eq. (1) was deemed necessary to provide a reasonable fit to $D_0(Z_{dr})_{fit}$ under a variety of $(D_{max})_{fit}$ assumptions that include the presence of large drops and resonant behavior in C-band Z_{dr} (Fig. 3). As pointed out by Bringi et al. (2006), there is no physical reason for $D_0(Z_{dr})_{fit}$ to take the more common form of a power law. Bringi et al. (2009) also employed high-order polynomial fits to estimate D_0 from C-band Z_{dr}. In this study, the order of the polynomial was raised until the overall D_0 retrieval error was subjectively minimized. Note that this study did not quantitatively explore the relative performance of various functions, including other functions besides for polynomials, for estimating D_0 from C-band Z_{dr}.

Last, for each experiment, a $(D_{max})_{truth}$ was postulated as the true maximum diameter for developing

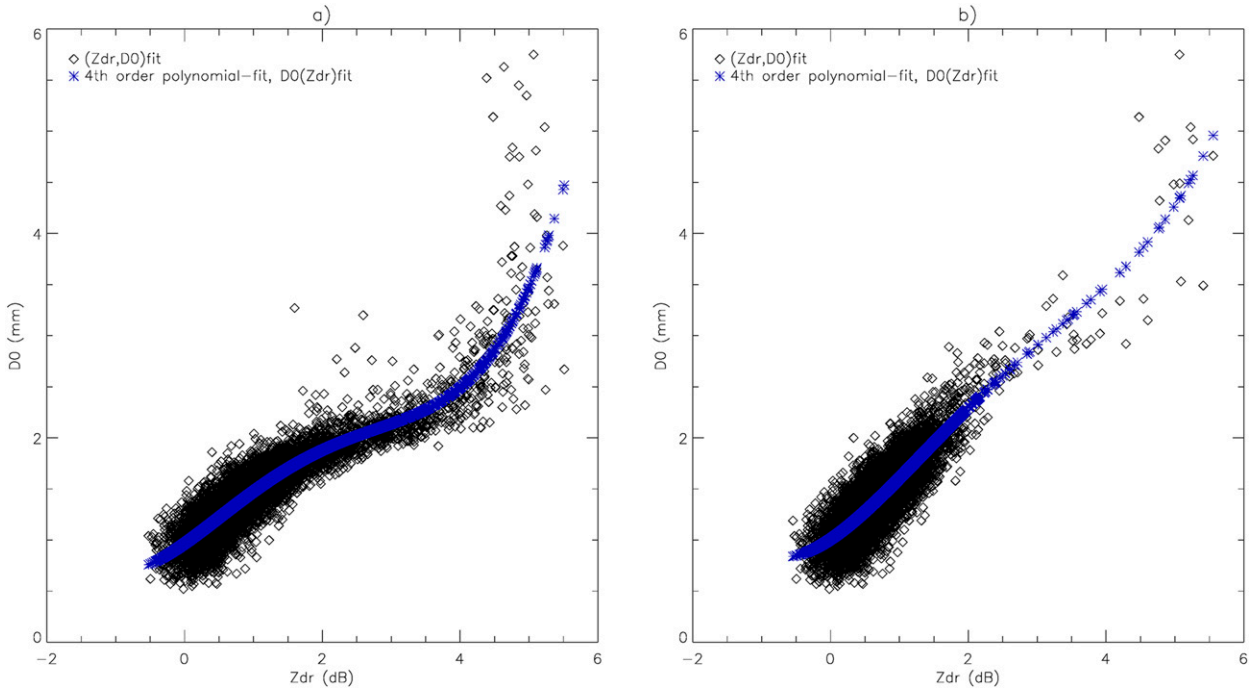

FIG. 3. Simulated median volume diameter (D_0; mm) vs the differential reflectivity (Z_{dr}; dB) at C band (black diamonds) and the best-fit fourth-order polynomial, $D_0(Z_{dr})_{fit}$ (blue asterisks), assuming (a) $(D_{max})_{fit} = 3.5D_0$ and (b) $(D_{max})_{fit} = 2D_0$. Note that the presence of negative Z_{dr} is associated with the inclusion of simulated Gaussian noise in Z_{dr}.

the truth dataset of $(D_0)_{truth}$ against which the polynomial fit in Eq. (1) was evaluated. The bias and standard errors of Eq. (1) were assessed as a function of the mismatch between the assumed $(D_{max})_{fit}$ for Eq. (1) and the postulated $(D_{max})_{truth}$. In this manner, the sensitivity of $D_0(Z_{dr})_{fit}$ to D_{max} assumptions was assessed. For both values of D_{max}, the truncated method of moments is used to develop the gamma triplet of parameters (N_0, D_0, μ). The quantity $(D_{max})_{fit}$ is used to derive $(N_0, D_0, \mu)_{fit}$, which are input to a radar scattering model to derive $(Z_{dr})_{fit}$ for the development of Eq. (1) or $D_0(Z_{dr})_{fit}$. Meanwhile, $(D_{max})_{truth}$ is used to derive $(N_0, D_0, \mu)_{truth}$, which are also input to the radar scattering model to derive $(Z_{dr})_{truth}$. To determine bias and standard error as a function of D_{max} assumptions, the performance of the $D_0(Z_{dr})_{fit}$ equation is evaluated against the $(D_0)_{truth}$ data.

The normalized bias (NB) and the normalized standard error (NSE) were used to evaluate the performance of the $D_0(Z_{dr})_{fit}$ estimator in Eq. (1) relative to $(D_0)_{truth}$ according to

$$\mathrm{NB} = \left\langle \frac{\sum\{[D_0(Z_{dr})_{fit}] - (D_0)_{truth}\}}{n} \right\rangle \Big/ (\overline{D}_0)_{truth} \quad \text{and} \tag{2}$$

$$\mathrm{NSE} = \left\langle \frac{\sum\{[D_0(Z_{dr})_{fit}] - [\overline{D}_0(Z_{dr})_{fit}] - (D_0)_{truth} + (\overline{D}_0)_{truth}\}^2}{n} \right\rangle^{1/2} \Big/ (\overline{D}_0)_{truth}, \tag{3}$$

where $D_0(Z_{dr})_{fit}$ is the estimated D_0 from polynomial fit in Eq. (1) that is associated with the assumed $(D_{max})_{fit}$, $(D_0)_{truth}$ is the postulated true D_0 that is associated with the postulated $(D_{max})_{truth}$, the overbar indicates a mean, and n is the number of samples.

3. Results and discussion

The results of the D_0 retrieval experiments are first overviewed by presenting the family of $D_0(Z_{dr})_{fit}$ polynomials at C band associated with varying the $(D_{max})_{fit}$

assumption through values typically found in the literature, as reviewed in section 1b. The potential overall bias and standard (i.e., scatter) errors of the D_0 retrievals and their sensitivity to D_{max} assumptions are then assessed by assuming a $(D_{max})_{fit}$ and evaluating the associated $D_0(Z_{dr})_{fit}$ polynomial against various truth datasets, $(D_0)_{truth}$, associated with a different postulated $(D_{max})_{truth}$. The D_0 retrieval errors associated with an incorrectly postulated D_{max} are also evaluated as a function of Z_{dr} and radar wavelength (X, C, and S band) to highlight the importance of resonant scattering. Finally, the potential impact of drop temperature is explored by conducting sensitivity tests at various drop temperatures.

a. Sensitivity of polarimetric D_0 retrieval to maximum diameter at C band

Examples of simulated pairs of (D_0, Z_{dr}) data at C band and the associated $D_0(Z_{dr})_{fit}$ best-fit polynomials for the assumptions of $D_{max} = 3.5D_0$ and $D_{max} = 2D_0$ can be found in Figs. 3a and 3b, respectively. As expected, D_0 increases monotonically with increasing C-band Z_{dr} with some scatter about a best-fit polynomial. The primary effect of increasing the assumed D_{max} from $2D_0$ to $3.5D_0$ is to flatten the $D_0(Z_{dr})_{fit}$ polynomial at moderate to large Z_{dr}. In other words, the simulated D_0 are systematically smaller at a given Z_{dr} for $D_{max} = 3.5D_0$ relative to $D_{max} = 2D_0$, particularly at moderate-to-large Z_{dr}.

To better understand the effect of D_{max} and the impact of resonant scattering at C band, the best-fit polynomials $D_0(Z_{dr})_{fit}$ assuming constant D_{max} varying from 4 to 10 mm are shown in Fig. 4a. At most values of Z_{dr}, the D_0 inferred from the best-fit polynomials decreases with the assumed $(D_{max})_{fit}$. A significant transition in the functionality of D_0 with respect to Z_{dr} occurs between the polynomials associated with $(D_{max})_{fit} = 5$ and 6 mm. The difference between the two polynomials is most obvious at moderate-to-large Z_{dr} (e.g., $1.5 < Z_{dr} < 3$ dB) where the inferred D_0 from the polynomial assuming $(D_{max})_{fit} = 5$ mm becomes increasingly larger than the D_0 inferred from the polynomial with $(D_{max})_{fit} = 6$ mm. The $D_0(Z_{dr})_{fit}$ polynomials for $(D_{max})_{fit} \geq 6$ mm tend to be much flatter with $Z_{dr} > 1.5$ dB than those for $(D_{max})_{fit} < 6$ mm. This significant transition in the $D_0(Z_{dr})_{fit}$ polynomial behavior with $(D_{max})_{fit}$ is associated with resonance scattering and the rapid increase in Z_{dr} for drops between 5 and 6 mm in diameter (Fig. 2).

Note that the $D_0(Z_{dr})_{fit}$ polynomial for $(D_{max})_{fit} = 5$ mm is only strictly valid to about $Z_{dr} = 3$ dB as values larger than this do not occur when $(D_{max})_{fit} = 5$ mm (Fig. 4a). Extrapolation of the best-fit polynomial associated with $(D_{max})_{fit} = 5$ mm to larger values of Z_{dr} would result in drastically larger estimated D_0 than the polynomial associated with $(D_{max})_{fit} = 6$ mm (or larger D_{max}). Similar conclusions can be drawn for the $D_0(Z_{dr})_{fit}$ polynomial associated with $(D_{max})_{fit} = 4$ mm, which is much closer in behavior to the polynomial for $(D_{max})_{fit} = 5$ mm than to $(D_{max})_{fit} \geq 6$ mm. Similarly, the $D_0(Z_{dr})_{fit}$ polynomial for $(D_{max})_{fit} = 6$ mm is much closer to those polynomials associated with $(D_{max})_{fit} \geq 7$ mm. In fact, there is very little difference in the estimated D_0 from the polynomials associated with $(D_{max})_{fit} \geq 7$ mm except at very large $Z_{dr} > 4$ dB.

It is worth noting that the behavior of the $D_0(Z_{dr})_{fit}$ polynomial for a $(D_{max})_{fit}$ given by the actual disdrometer-measured D_{max} is very close to the polynomials for $(D_{max})_{fit} = 4$–5 mm for $Z_{dr} \leq 2.25$ dB and then rapidly deviates as those polynomials curve upward to large D_0 for increasing Z_{dr} (Fig. 4a). For $Z_{dr} > 2.25$ dB, the $D_0(Z_{dr})_{fit}$ polynomial associated with the actual 2DVD-measured D_{max} remains relatively flat similar to the polynomials for $(D_{max})_{fit} \geq 6$ mm but falling at a noticeably larger D_0 for a given Z_{dr} up to about 4.5 dB.

By assuming a constant $(D_{max})_{fit}$ varying from 4 to 10 mm, it is clear that 1) increasing $(D_{max})_{fit}$ results in generally smaller estimated $D_0(Z_{dr})_{fit}$ for a given Z_{dr} (up to about 4.5 dB), and 2) resonance scattering causes a dramatic decrease in the inferred $D_0(Z_{dr})_{fit}$ at $Z_{dr} > 1.5$ dB for all polynomials having $(D_{max})_{fit} \geq 6$ mm. However, assuming a constant D_{max} for all DSDs is not physically realistic, is not consistent with the 2DVD measurements in Fig. 1 and is not in keeping with many previous studies (section 1b).

To simulate more realistic $D_0(Z_{dr})_{fit}$ polynomials and test a range of assumptions utilized in the literature, $(D_{max})_{fit}$ was started at $2D_0$, which is the mean value for the DSD dataset utilized in this study, and increased to $2.5D_0$, then $3D_0$ and finally $3.5D_0$, which have all been utilized in the literature to retrieve polarimetric radar-based DSD equations (e.g., Fig. 1; Keenan et al. 2001; Bringi et al. 2002, 2003, 2006, 2009; Thurai et al. 2007). The resulting $D_0(Z_{dr})_{fit}$ polynomials are provided in Fig. 4b along with the $D_0(Z_{dr})_{fit}$ polynomials associated with $4D_0$ and the actual 2DVD-measured D_{max} for reference. The coefficients of the corresponding fourth-order polynomials [Eq. (1)] can be found in Table 1.

As noted for constant D_{max}, the estimated D_0 from the $D_0(Z_{dr})_{fit}$ polynomials for a given Z_{dr} decreases with increasing $(D_{max})_{fit} = CD_0$ (i.e., with increasing C) (Fig. 4b). The differences between the various $D_0(Z_{dr})_{fit}$ polynomials are particularly noticeable at $Z_{dr} > 1.5$ dB. As $(D_{max})_{fit} = CD_0$ (i.e., C) increases, the $D_0(Z_{dr})_{fit}$ polynomials become increasingly flatter at $1.5 < Z_{dr} < 4$ dB, resulting in a significantly lower estimated D_0 for

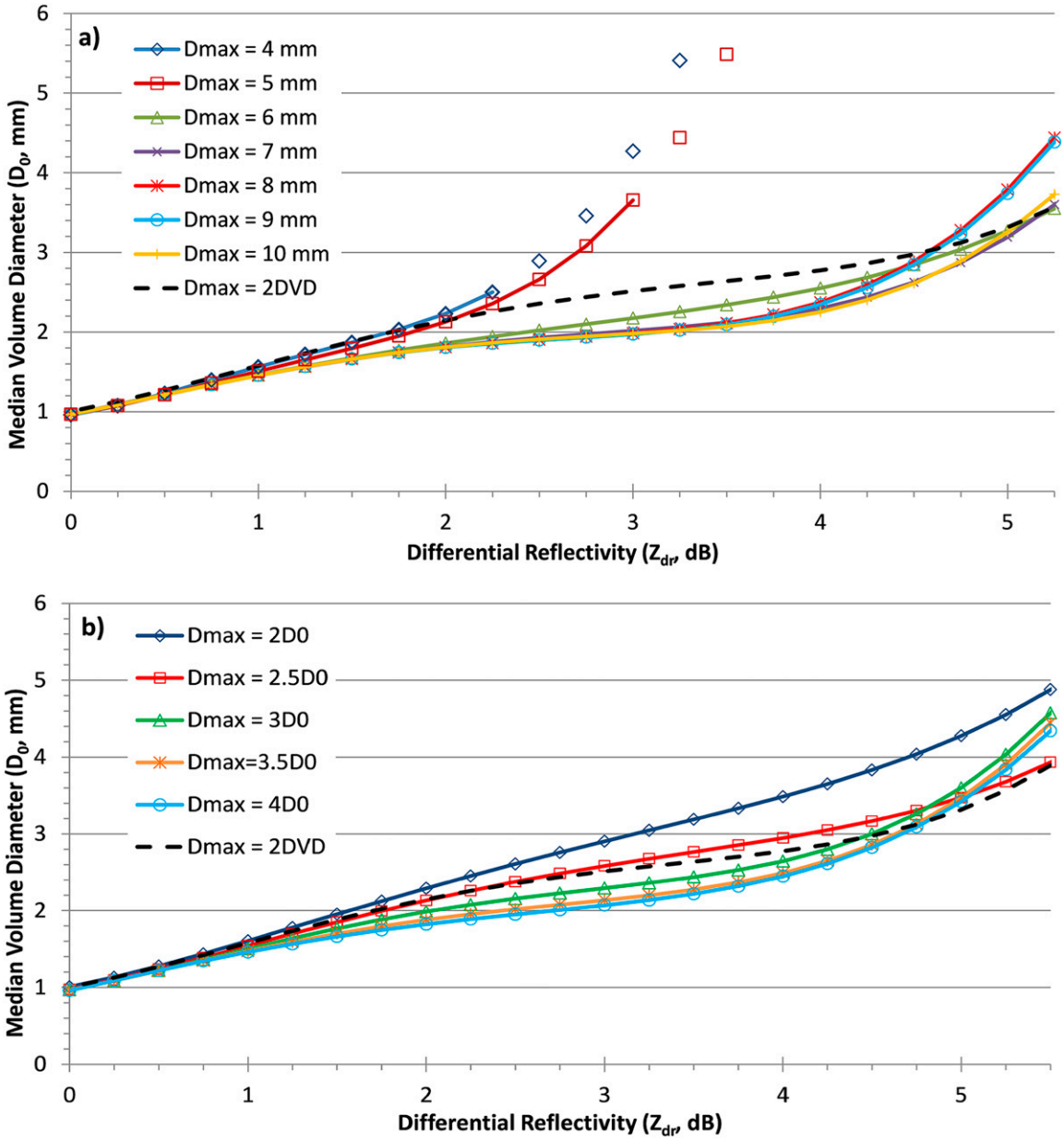

FIG. 4. The simulated median volume diameter (D_0; mm) vs the simulated differential reflectivity (Z_{dr}; dB) at C band derived from observed DSD data. Each curve represents a fourth-order polynomial fit to simulated pairs of (Z_{dr}, D_0) with a different assumption regarding the maximum raindrop size $(D_{max})_{fit}$. (a) D_{max} is assumed constant [$(D_{max})_{fit}$ = 4, 5, 6, 7, 8, 9, or 10 mm as shown]. For $(D_{max})_{fit}$ = 4 and 5 mm, markers not accompanied by a plotted curve represent an extrapolation of the polynomial fit beyond the maximum simulated Z_{dr}. (b) D_{max} is assumed to be a multiple of D_0 [$(D_{max})_{fit} = 2D_0$, $2.5D_0$, $3D_0$, $3.5D_0$, and $4D_0$ as shown]. In both (a) and (b), the dashed line represents the polynomial fit of D_0 vs Z_{dr} for the actual observed 2DVD maximum. Polynomial coefficients for the curves in (b) can be found in Table 1. The remaining assumptions and methods for deriving the simulated pairs of (Z_{dr}, D_0) at C band from observed DSD data are discussed in section 2.

a given Z_{dr}. The difference between adjacent $D_0(Z_{dr})_{fit}$ polynomials in the family of $(D_{max})_{fit} = CD_0$ curves becomes smaller as C increases. In other words, the difference between $(D_{max})_{fit} = 2D_0$ and $2.5D_0$ is larger than the difference between $3D_0$ and $3.5D_0$. In fact, there is very little difference between assuming $(D_{max})_{fit} = 3.5D_0$ and $4D_0$. The $D_0(Z_{dr})_{fit}$ polynomial associated with a $(D_{max})_{fit}$ equal to the measured 2DVD D_{max} is more similar to $(D_{max})_{fit} = 2D_0$ at small Z_{dr} (although it is difficult to see that in Fig. 4b) and most similar to

TABLE 1. Coefficients (a, b, c, d, and e) of the fourth-order polynomial for $D_0(Z_{dr})_{fit}$ as shown in Eq. (1) for C band. The coefficients were obtained from a nonlinear least squares curve fit to pairs of simulated (Z_{dr}, D_0) for various D_{max} assumptions at C band. Methods and assumptions for developing the simulation dataset are discussed in section 2.

D_{max}	a	b	c	d	e
$2D_0$	0.008 313	−0.076 431	0.214 788	0.451 232	1.008 394
$2.5D_0$	0.008 569	−0.077 835	0.184 387	0.452 424	0.975 656
$3D_0$	0.014 309	−0.106 806	0.195 715	0.429 318	0.969 980
$3.5D_0$	0.011 978	−0.079 173	0.101 970	0.473 660	0.966 161
$4D_0$	0.009 219	−0.051 395	0.020 882	0.520 548	0.961 739
2DVD measured	0.012 073	−0.104 753	0.226 222	0.440 944	1.005 231

$(D_{max})_{fit} = 2.5D_0$ through a broad range of Z_{dr} from 1 to 4 dB.

b. Overall D_0 retrieval error

To assess the overall D_0 retrieval error, each $D_0(Z_{dr})_{fit}$ polynomial associated with an assumed $(D_{max})_{fit}$ was evaluated against a $(D_0)_{truth}$ dataset associated with a postulated $(D_{max})_{truth}$. To visualize this kind of test in Fig. 5a, the pairs of $(Z_{dr}, D_0)_{fit}$ data used for derivation of the $D_0(Z_{dr})_{fit}$ polynomial assuming $(D_{max})_{fit} = 3.5D_0$ are accompanied by pairs of true $(Z_{dr}, D_0)_{truth}$ assuming $(D_{max})_{truth} = 2D_0$, which is close to observed (Fig. 1). In this example, it is clear that the $D_0(Z_{dr})_{fit}$ polynomial assuming $(D_{max})_{fit} = 3.5D_0$ is underestimating the true D_0, $(D_0)_{truth}$, at a given Z_{dr} assuming $(D_{max})_{truth} = 2D_0$. The "fit" and "truth" datasets are then reversed in Fig. 5b. Correspondingly, it is easy to see how the $D_0(Z_{dr})_{fit}$ polynomial assuming $(D_{max})_{fit} = 2D_0$ is overestimating the true D_0, $(D_0)_{truth}$, at a given Z_{dr} assuming $(D_{max})_{truth} = 3.5D_0$.

Normalized bias errors for various $D_0(Z_{dr})_{fit}$ polynomials assuming constant $(D_{max})_{fit}$ from 4 to 10 mm across the entire sample of $(Z_{dr}, D_0)_{truth}$ assuming various $(D_{max})_{truth}$ are provided in Fig. 6. For $(D_{max})_{fit} \geq 6$ mm and $(D_{max})_{truth} \geq 6$ mm, the absolute normalized bias errors of $D_0(Z_{dr})_{fit}$ are small (<3%). For $(D_{max})_{fit} \geq 6$ mm and $(D_{max})_{truth} < 6$ mm, the normalized bias errors of $D_0(Z_{dr})_{fit}$ range from −4.2% to −5.9%. Compared to a $(D_{max})_{truth}$ equal to the 2DVD-measured D_{max}, the normalized bias errors for $D_0(Z_{dr})_{fit}$ assuming

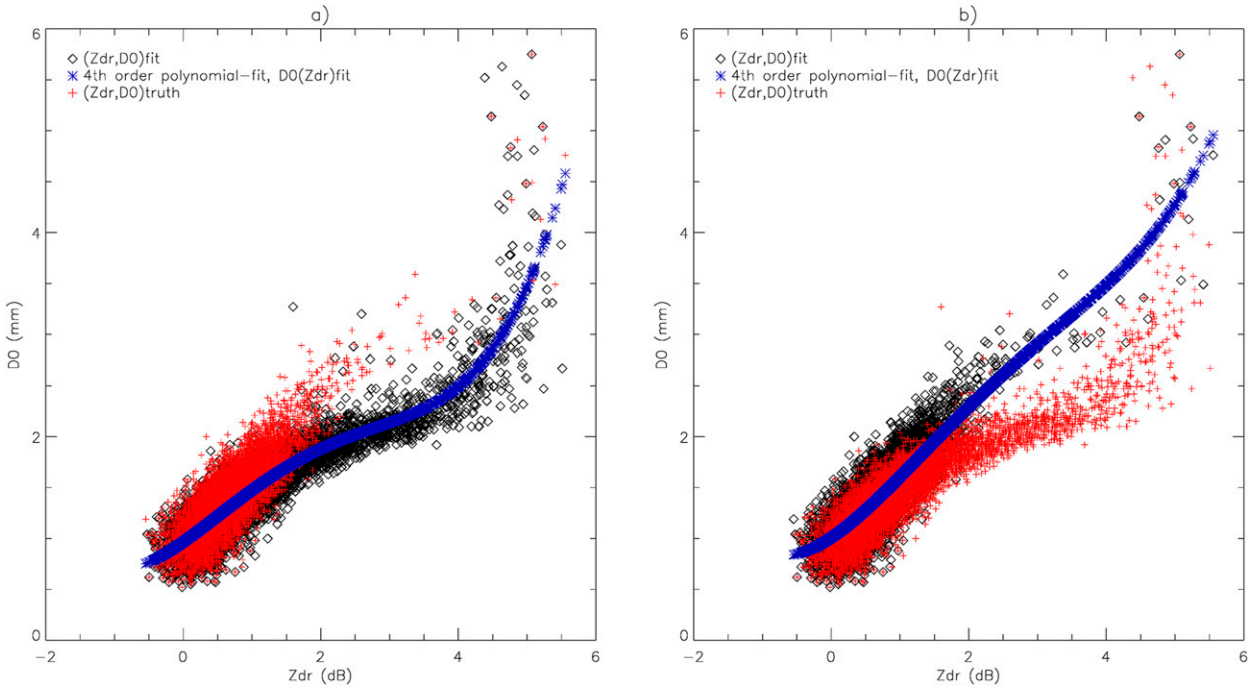

FIG. 5. As in Fig. 3, but (a) the pairs of $(Z_{dr}, D_0)_{fit}$ data (black diamonds) used for derivation of the best-fit fourth-order polynomial [$D_0(Z_{dr})_{fit}$; asterisks] assuming $(D_{max})_{fit} = 3.5D_0$ are accompanied by pairs of true $(Z_{dr}, D_0)_{truth}$ (red pluses) assuming $(D_{max})_{truth} = 2D_0$, and (b) the pairs of $(Z_{dr}, D_0)_{fit}$ data (black diamonds) used for derivation of the best-fit fourth-order polynomial [$D_0(Z_{dr})_{fit}$; asterisks] assuming $(D_{max})_{fit} = 2D_0$ are accompanied by pairs of true $(Z_{dr}, D_0)_{truth}$ (red pluses) assuming $(D_{max})_{truth} = 3.5D_0$. Note that the "fit" (black diamonds) and "truth" (red pluses) (Z_{dr}, D_0) datasets are simply reversed between (a) and (b).

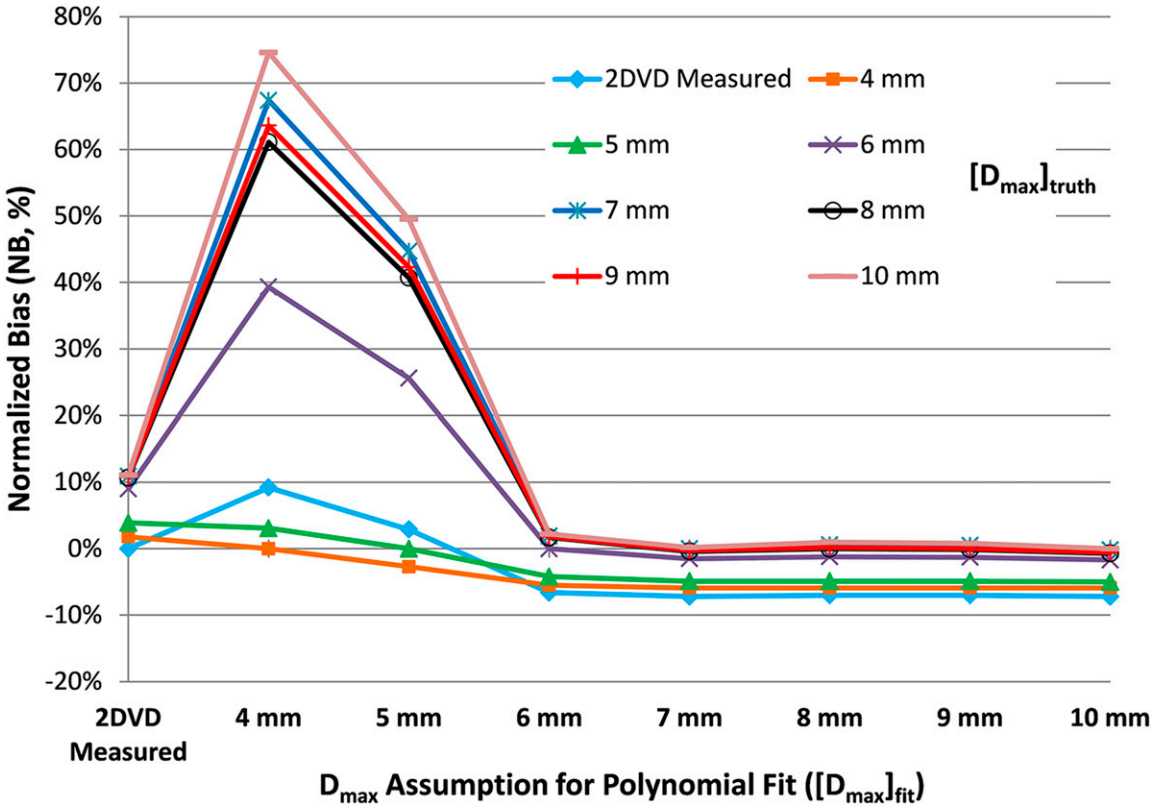

FIG. 6. The NB (%) of the median volume diameter estimated from the best-fit polynomial, $D_0(Z_{dr})_{fit}$, assuming the $(D_{max})_{fit}$ in the abscissa, relative to a true dataset, $(Z_{dr}, D_0)_{truth}$, with an assumed $(D_{max})_{truth}$. Each colored curve represents the NB of $D_0(Z_{dr})_{fit}$ relative to a different truth dataset, $(Z_{dr}, D_0)_{truth}$, assuming the indicated $(D_{max})_{truth}$ while all else is held equal. The quantity D_{max} is assumed constant at different values (D_{max} = 4, 5, 6, 7, 8, 9, and 10 mm) or set to the actual 2DVD-measured D_{max} as shown.

$(D_{max})_{fit} \geq 6$ mm are approximately −7%. If $(D_{max})_{fit} <$ 6 mm and $(D_{max})_{truth} <$ 6 mm, then the absolute normalized bias errors of $D_0(Z_{dr})_{fit}$ are fairly small (<4%). If $(D_{max})_{fit} <$ 6 mm and $(D_{max})_{truth}$ is equal to the 2DVD-measured D_{max}, then the normalized bias errors of $D_0(Z_{dr})_{fit}$ range approximately from 3% to 9%. On the other hand, if $(D_{max})_{fit} <$ 6 mm and $(D_{max})_{truth} >$ 6 mm, then the normalized bias errors of $D_0(Z_{dr})_{fit}$ are extremely large, ranging from 26% to 75%, and are largely the result of resonant scattering on the truth dataset and of extrapolating the $D_0(Z_{dr})_{fit}$ polynomials to larger values of Z_{dr} that are not present in the fit dataset but are in the truth dataset (Fig. 4a). These very large values of normalized bias error are likely not realistic since D_{max} is likely not constant for all DSD but Fig. 6 does emphasize the potential effect of resonance on the bias error associated with retrieving D_0 using C-band Z_{dr} associated with assuming an inappropriate D_{max}.

To provide a more realistic assessment of bias error, the normalized bias errors for various $D_0(Z_{dr})_{fit}$ polynomials assuming $(D_{max})_{fit} = CD_0$ (C = 2–4) across the entire sample of $(D_0)_{truth}$ assuming various $(D_{max})_{truth} = CD_0$ (C = 2–4) are provided in Fig. 7. Despite the known sampling limitations of disdrometers, the actual 2DVD-measured D_{max} is also utilized as a potentially realistic $(D_{max})_{fit}$ and $(D_{max})_{truth}$. As shown by the statistics of D_{max}/D_0 in Fig. 1a and other studies (Keenan et al. 2001; Gatlin et al. 2015), this range of C and hence D_{max} should adequately represent a potential realistic range of D_{max} when considering potential undersampling of large drops by the 2DVD. As a result, the range of normalized bias errors in Fig. 7 should bracket the overall bias errors potentially present in recent D_0 retrieval studies using Z_{dr} associated with potential misalignment of the assumed and actual D_{max}. Because the $(D_{max})_{fit} = 2D_0$ polynomial is the most different than the others (Fig. 4b), its range of possible normalized bias errors for $D_0(Z_{dr})_{fit}$ is the largest (0%–16%). The possible range of normalized bias errors for $D_0(Z_{dr})_{fit}$ decreases as $(D_{max})_{fit}$ increases from $2D_0$ to $4D_0$. For $(D_{max})_{fit} = 2.5D_0$, the possible normalized bias error for $D_0(Z_{dr})_{fit}$ ranges from −2% to 9%. As expected from Fig. 4b, the range of possible bias error for $D_0(Z_{dr})_{fit}$ assuming a $(D_{max})_{fit}$ of the measured 2DVD D_{max} falls between $(D_{max})_{fit} = 2D_0$ and $2.5D_0$. For $(D_{max})_{fit} = 3D_0$ ($4D_0$), the possible

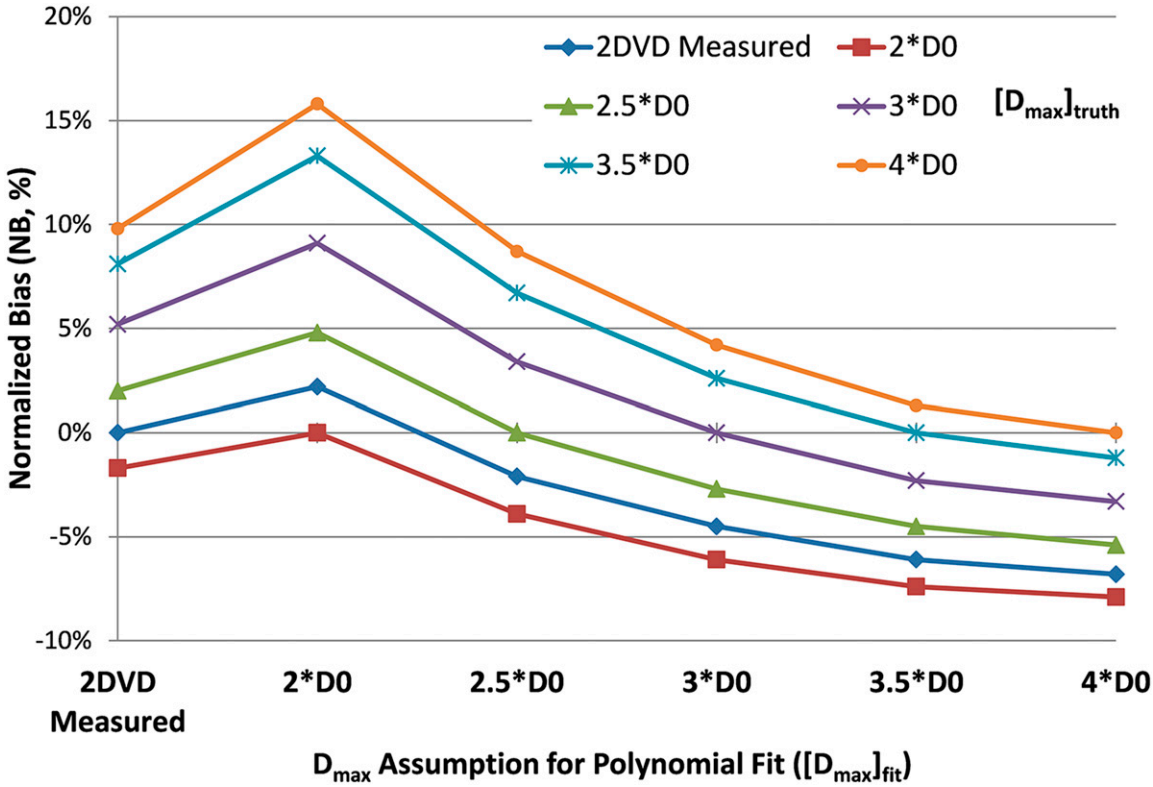

FIG. 7. As in Fig. 6, but D_{max} is assumed to be a multiple of D_0 ($D_{max} = 2D_0, 2.5D_0, 3D_0, 3.5D_0, 4D_0$) or set to the actual 2DVD-measured D_{max} as shown.

normalized bias error ranges from −6% to 4% (−8% to 0%). As summarized in section 1a, the absolute normalized bias error for D_0 in past studies has typically been estimated to be less than 5%. The results herein demonstrate that the absolute normalized bias error for estimating D_0 using C-band Z_{dr} could be 2–3 times as large (i.e., 10%–15%) as previously estimated (section 1a) because of a potential error in the

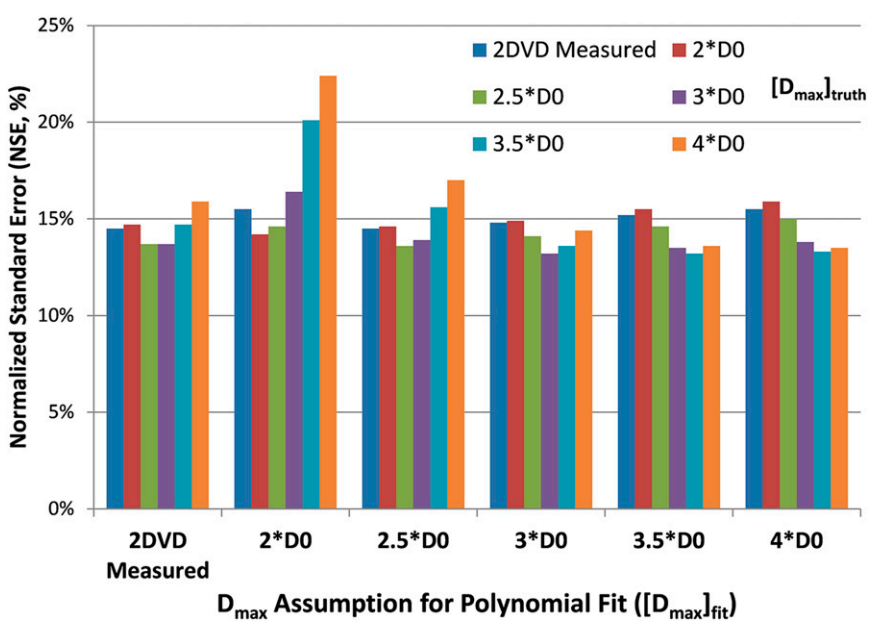

FIG. 8. As in Fig. 7, but the NSE (%) is depicted.

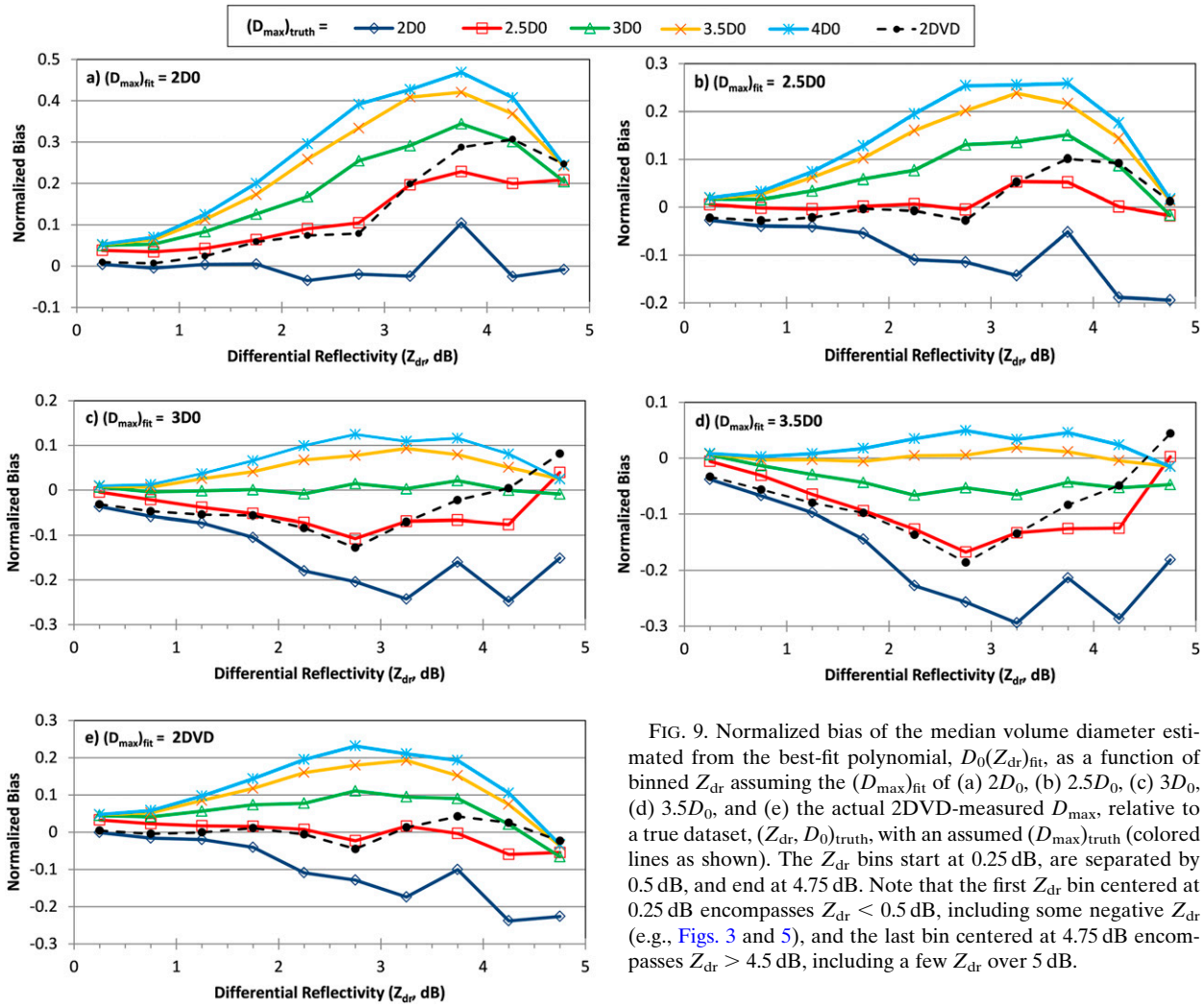

FIG. 9. Normalized bias of the median volume diameter estimated from the best-fit polynomial, $D_0(Z_{dr})_{fit}$, as a function of binned Z_{dr} assuming the $(D_{max})_{fit}$ of (a) $2D_0$, (b) $2.5D_0$, (c) $3D_0$, (d) $3.5D_0$, and (e) the actual 2DVD-measured D_{max}, relative to a true dataset, $(Z_{dr}, D_0)_{truth}$, with an assumed $(D_{max})_{truth}$ (colored lines as shown). The Z_{dr} bins start at 0.25 dB, are separated by 0.5 dB, and end at 4.75 dB. Note that the first Z_{dr} bin centered at 0.25 dB encompasses $Z_{dr} < 0.5$ dB, including some negative Z_{dr} (e.g., Figs. 3 and 5), and the last bin centered at 4.75 dB encompasses $Z_{dr} > 4.5$ dB, including a few Z_{dr} over 5 dB.

assumed maximum drop diameter. Of course, the overall bias error depends on the degree of mismatch between the assumed and true D_{max} and many (61%) of the tested scenarios in Fig. 7 have normalized bias errors falling within ±5%.

Since the major effect of varying C from 2 to 4 in $(D_{max})_{fit} = CD_0$ on the $D_0(Z_{dr})_{fit}$ polynomials is to shift the $D_0(Z_{dr})_{fit}$ polynomial upward and downward (Fig. 4b), it was hypothesized that the normalized standard error would not vary dramatically because of a mismatch between the assumed $(D_{max})_{fit}$ and $(D_{max})_{truth}$. Because there is a minor change in the shape of the polynomial with varying $(D_{max})_{fit}$ that is most apparent for $(D_{max})_{fit} = 2D_0$ relative to the others (Fig. 4b), it was anticipated that its potential range of normalized error would be the largest. Results for the normalized standard error generally confirm these expectations (Fig. 8). For $(D_{max})_{fit} = 2D_0$, the normalized standard error for $D_0(Z_{dr})_{fit}$ ranges from 14% to 22%, which is somewhat larger than found in past studies (7%–15%) as noted in section 1a. For the other tested $(D_{max})_{fit}$ in Fig. 8, the normalized standard error for $D_0(Z_{dr})_{fit}$ varied between 14% and 17%, which is on the high end but generally consistent with these past studies. In this study, the standard error of Z_{dr} is assumed to be 0.25 dB, which is consistent with the standard deviation of Z_{dr} in vertically pointing ARMOR scans of drizzle. While reasonable for ARMOR, this standard error of Z_{dr} may be slightly higher than assumed in some prior studies, which could account for some of the difference in the normalized standard error for $D_0(Z_{dr})_{fit}$.

c. D_0 retrieval error as a function of differential reflectivity

Of course, bias and standard errors over the entire sample only tell part of the story. It is important to understand how errors in the estimated D_0 might vary as a function of the independently measured radar property,

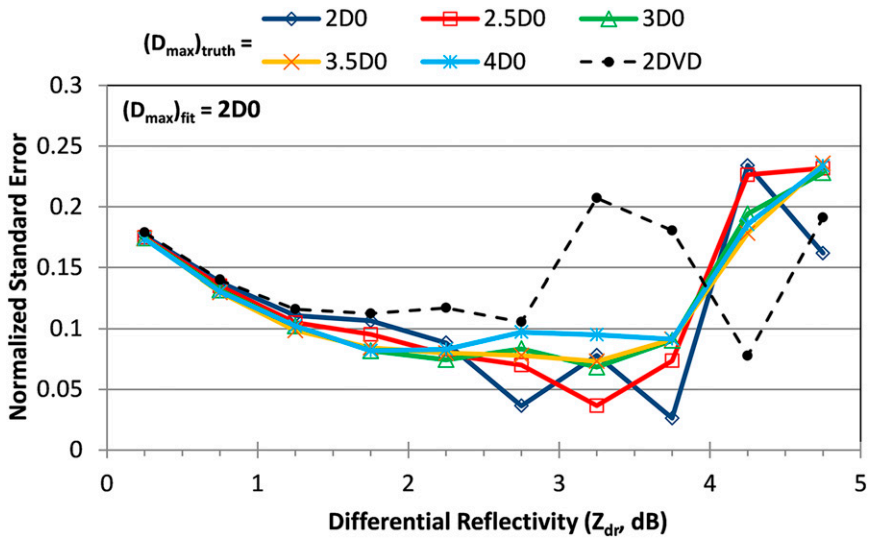

FIG. 10. As in Fig. 9a, but for the NSE of the median volume diameter estimated from the best-fit polynomial, $D_0(Z_{dr})_{fit}$. Results for only $(D_{max})_{fit} = 2D_0$ are given because the results for other assumed $(D_{max})_{fit}$ do not vary noticeably from what is presented here. In other words, the NSE of $D_0(Z_{dr})_{fit}$ as a function of Z_{dr} is not strongly dependent on the assumed $(D_{max})_{fit}$.

in this case Z_{dr}. As such, the normalized bias error is presented in Figs. 9a–e as a function of Z_{dr} for the same range of assumptions for $(D_{max})_{fit} = CD_0$ (C = 2–3.5) or the measured 2DVD D_{max}. In each panel of Figs. 9a–e, the $(D_{max})_{truth}$, each represented by a different curve, is varied through a similar range of D_{max} [i.e., $(D_{max})_{truth} = CD_0$ (C = 2–4) or the measured 2DVD D_{max}]. The largest normalized bias errors for $D_0(Z_{dr})_{fit}$ can be found at the two extremes of the assumed $(D_{max})_{fit}$, which are $(D_{max})_{fit} = 2D_0$ (Fig. 9a) and $3.5D_0$ (Fig. 9d). For $(D_{max})_{fit} = 2D_0$, the normalized bias error for $D_0(Z_{dr})_{fit}$ can exceed 0.1 for Z_{dr} as low as 1–1.5 dB and can increase from there to values as large as 0.23–0.47 for larger Z_{dr}, depending on the degree of mismatch between the assumed $(D_{max})_{fit}$ and $(D_{max})_{truth}$. Of course, if $(D_{max})_{fit}$ and $(D_{max})_{truth}$ are well aligned, then the bias errors with Z_{dr} are generally smaller. Similarly, for $(D_{max})_{fit} = 3.5D_0$, the absolute normalized bias error for $D_0(Z_{dr})_{fit}$ can reach 0.1 for Z_{dr} as low as 1–1.75 dB and can increase from there to values as large as 0.17–0.29 for larger Z_{dr} when the mismatch between the assumed $(D_{max})_{fit}$ and $(D_{max})_{truth}$ is large [e.g., see the curves for $(D_{max})_{truth} = 2D_0$, $2.5D_0$ and the 2DVD-measured value in Fig. 9d].

Absolute normalized bias errors for $D_0(Z_{dr})_{fit}$ larger than 0.1 can be found at $Z_{dr} > 1.5$ dB for all assumed $(D_{max})_{fit}$ in Figs. 9a–e depending on the misalignment with $(D_{max})_{truth}$. Even if it is assumed that $D_{max}/D_0 \geq 2.5$ always, which may or may not be realistic as highlighted in Fig. 1a and earlier discussion, the absolute normalized bias error can still exceed 0.1 at Z_{dr} as low as 1.75 dB (Fig. 9b), which is associated with a D_0 of 1.7–2.0 mm (Fig. 4b). Clearly, the relationship between D_0 and C-band Z_{dr} for a gamma DSD is not relatively insensitive to changes in D_{max}/D_0 for values of $D_0 \leq 3.2$ mm provided $D_{max}/D_0 \geq 2.5$ as found by Ulbrich and Atlas (1984) for S-band Z_{dr} in their study. This difference with the S band results in Ulbrich and Atlas (1984) is due in part to the effect of resonance on C-band Z_{dr} in large drops greater than 5 mm in diameter (Fig. 2), although differences in methodology and data may also play some role.

As shown in Fig. 10, the normalized standard error for $D_0(Z_{dr})_{fit}$ tends to be a maximum at both small Z_{dr} (<1.5 dB) and very large Z_{dr} (>4 dB). In between a Z_{dr} of 1.5 and 4 dB, the normalized standard errors of $D_0(Z_{dr})_{fit}$ tend to be <0.1. One exception is for an assumed $(D_{max})_{truth}$ equal to the 2DVD-measured D_{max}. The elevated values (>0.1) of normalized standard error at $Z_{dr} < 1.5$ dB are due in large part to the effect of random noise on Z_{dr}. For $Z_{dr} > 4$ dB, the sample size is relatively small and the parameterization error for $D_0(Z_{dr})_{fit}$ is likely larger (e.g., Fig. 3). The assumed D_{max} does not generally have a large effect on the variation of the normalized standard error with Z_{dr}.

d. Wavelength dependence of D_0 retrieval error

To explore the wavelength dependence of these results while holding all else equal, the normalized bias of $D_0(Z_{dr})_{fit}$ as a function of Z_{dr} for two different extreme D_{max} mismatch scenarios is shown in Fig. 11 for X, C, and S band: (i) $(D_{max})_{fit} = 3.5D_0$ and $(D_{max})_{truth} = 2D_0$ (Fig. 11a), and (ii) $(D_{max})_{fit} = 2D_0$ and $(D_{max})_{truth} = 3.5D_0$ (Fig. 11b). In both scenarios, the absolute normalized bias

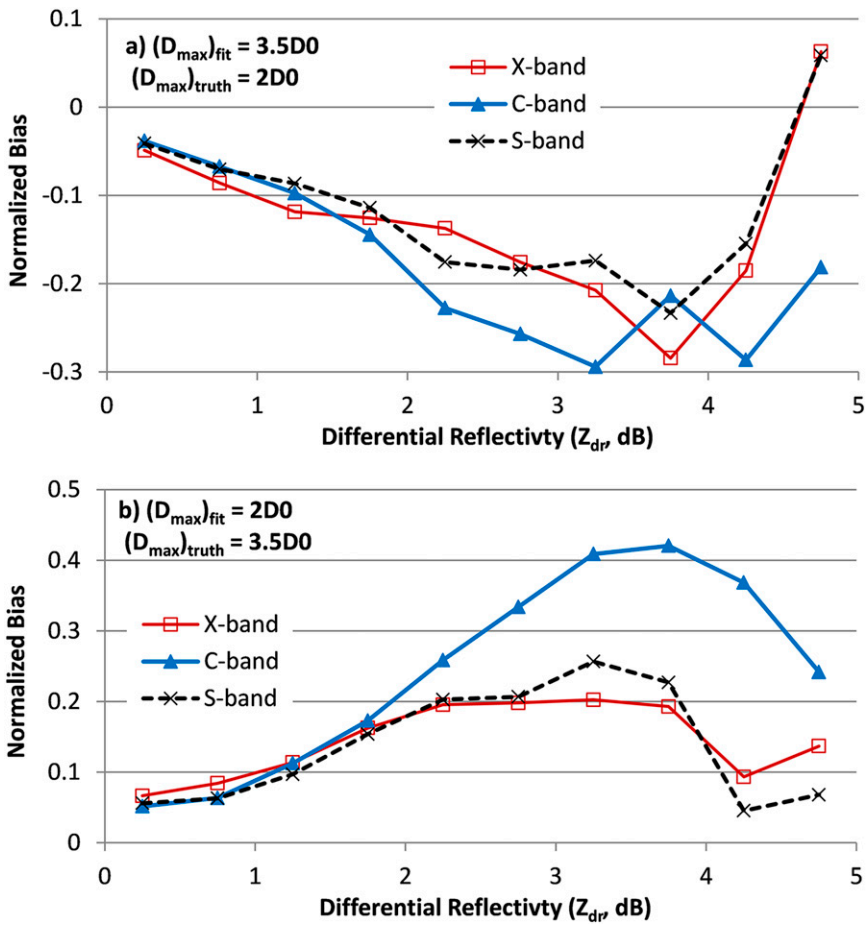

FIG. 11. As in Fig. 9, but adding results at X band and S band to the C band shown earlier for (a) $(D_{max})_{fit} = 3.5D_0$ and $(D_{max})_{truth} = 2D_0$ (cf. Fig. 9d) and (b) $(D_{max})_{fit} = 2D_0$ and $(D_{max})_{truth} = 3.5D_0$ (cf. Fig. 9a).

for $D_0(Z_{dr})_{fit}$ at X band slightly exceeds that of C and S band for $Z_{dr} < 1.5$ dB, which is associated with the slight impact of resonance on X-band Z_{dr} between a drop diameter of 3 and 4 mm (Fig. 2). For $Z_{dr} \geq 1.5$ dB, the absolute normalized bias for $D_0(Z_{dr})_{fit}$ at C band exceeds X and S band (with one minor exception at $Z_{dr} = 3.75$ dB in Fig. 11a). In fact, the absolute normalized bias error for $D_0(Z_{dr})_{fit}$ at C band can be significantly larger than at S band by as much as 0.12–0.13 for $Z_{dr} > 3$ dB in Fig. 11a and 0.13–0.32 for $Z_{dr} > 2.5$ dB in Fig. 11b. This difference in the bias error of the D_0 estimate between C-band Z_{dr} and S-band Z_{dr} is due to the effect of resonance on C-band Z_{dr} in large (>5 mm) raindrops (Fig. 2).

e. *Temperature dependence of D_0 retrieval error*

The impact of T was explored by conducting additional sensitivity tests at drop temperature of $T = 10°C$ and $T = 30°C$ in addition to the standard temperature of $T = 20°C$. The values of Z_{dr} at $T = 10°C$ and Z_{dr} at $T = 30°C$ are now compared with Z_{dr} at $T = 20°C$ in Figs. 12a and 12b, respectively. At larger values of Z_{dr}, (Z_{dr} at $T = 10°C$) < (Z_{dr} at $T = 20°C$) while it is reversed when the temperature is increased [i.e., (Z_{dr} at $T = 30°C$) > (Z_{dr} at $T = 20°C$)]. In other words, resonance has a larger impact on increasing C-band Z_{dr} at warmer temperatures. The impact of varying temperature on $D_0(Z_{dr})_{fit}$ was explored for a variety of D_{max} assumptions. The results are shown in Fig. 13 for $D_{max} = 3.5D_0$ since the results for other D_{max} assumptions were comparable. As expected from Fig. 12, at larger Z_{dr}, there is a negative bias in $D_0(Z_{dr})_{fit}$ for a temperature that is colder in truth ($T_{truth} = 10°C$) than what was assumed in developing the fit equation ($T_{fit} = 20°C$) (Fig. 13) while there is a positive bias in $D_0(Z_{dr})_{fit}$ for a temperature that is warmer in truth ($T_{truth} = 30°C$) than what was assumed in developing the fit equation ($T_{fit} = 20°C$) (Fig. 13). For a fairly large temperature mismatch of 10°C, the overall bias of $D_0(Z_{dr})_{fit}$ is negligible (≈0 dB) in the mean over the full range of Z_{dr} (i.e., for all DSDs). For larger Z_{dr} values, the $D_0(Z_{dr})_{fit}$ bias error can approach ±5%–10% for

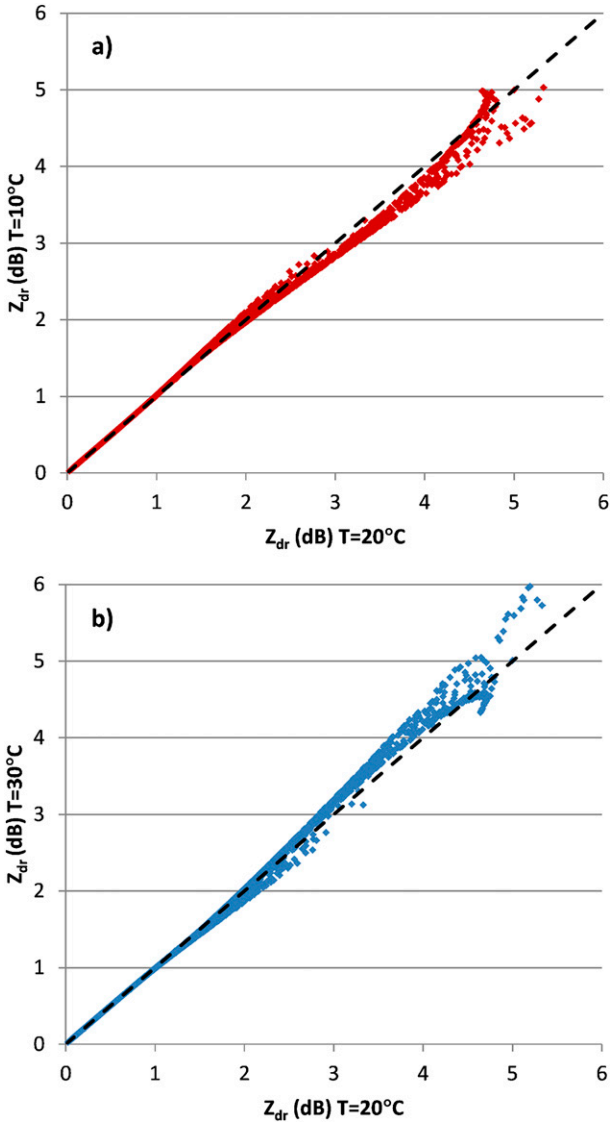

FIG. 12. A comparison of differential reflectivity (Z_{dr}; dB) simulated at different drop temperatures: (a) Z_{dr} at T = 10°C and (b) Z_{dr} at T = 30°C vs Z_{dr} at T = 20°C, which was the standard drop temperature assumption throughout the rest of the study. The maximum drop diameter was assumed to be $D_{max} = 3.5D_0$ for this temperature sensitivity test. The radar wavelength was C band. All other rain properties were as discussed in section 2a.

a temperature bias of ±10°C (Fig. 13). While these errors are not trivial, it is worthwhile to note that the impact of D_{max} uncertainty is likely often larger than the impact of temperature uncertainty on the accuracy of the $D_0(Z_{dr})_{fit}$ estimator (cf. Figs. 9 and 13).

4. Conclusions

Estimating the raindrop size, including median volume diameter, has been a long-standing objective of polarimetric radar–based precipitation retrieval methods, particularly those using the differential reflectivity. Theoretically, Z_{dr} is a measure of the reflectivity-factor-weighted mean axis ratio and therefore indirectly the reflectivity-factor-weighted drop size via the assumption of a drop size relation (Jameson 1983; Bringi and Chandrasekar 2001, p. 398). The theoretical relationship between Z_{dr} and D_0 (or D_m) is more complex and requires more assumptions regarding the DSD (e.g., Bringi and Chandrasekar 2001, p. 398). From a practical perspective, the relationship between Z_{dr} and D_0 is typically derived empirically using rain DSD observations from a disdrometer such as the 2DVD, a raindrop physical model, and a radar scattering model. Because disdrometers are known to undersample large raindrops and therefore underestimate the maximum raindrop size, D_{max} is often an assumed parameter in the rain physical model. Because there is remaining uncertainty regarding the appropriate D_{max} for a given DSD (Fig. 1), there have been a wide variety of assumptions for D_{max}. Because D_{max} affects the tail of the DSD and Z_{dr} is reflectivity weighted (i.e., D^6 for Rayleigh–Gans scattering), variability in the D_{max} assumption can affect the relationship between Z_{dr} and D_0, as was noted in early studies such as Ulbrich and Atlas (1984) at S band.

Although there have been a number of DSD retrieval application studies at C band, the sensitivity of the relationship between Z_{dr} and D_0 to D_{max} and the associated potential error in the retrieved D_0 have not been investigated in any detail. C-band polarimetric radars are commonly used in research and operations worldwide because of their decreased cost relative to S band. Compared to S band, C band has some complicating factors to consider before analysis of raindrop properties, including increased propagation effects and resonance scattering (or non-Rayleigh–Gans scattering) in large raindrops (i.e., diameter > 5 mm). Resonance scattering can complicate the relationship between the Z_{dr} and diameter of individual raindrops (Fig. 2) and between Z_{dr} and D_0 (Fig. 4) of realistic DSDs with an assumed D_{max}.

In this study, a series of experiments were conducted that postulate a $(D_{max})_{fit}$ for the fitting of a fourth-order polynomial to $(Z_{dr}, D_0)_{fit}$ data derived from 2DVD data, a rain model, and a radar scattering model at C band. The resulting $D_0(Z_{dr})_{fit}$ polynomial, which is associated with an assumed $(D_{max})_{fit}$, was then compared with a truth dataset, $(D_0)_{truth}$, which is associated with an assumed $(D_{max})_{truth}$ (Fig. 5). The normalized bias and scatter errors for $D_0(Z_{dr})_{fit}$ relative to $(D_0)_{truth}$ were then computed while varying both $(D_{max})_{fit}$ and $(D_{max})_{truth}$ through the range of assumptions found in the literature.

It is found that the overall absolute normalized bias errors for $D_0(Z_{dr})_{fit}$ can be as high as 10%–15% at C band depending on the degree of mismatch between the

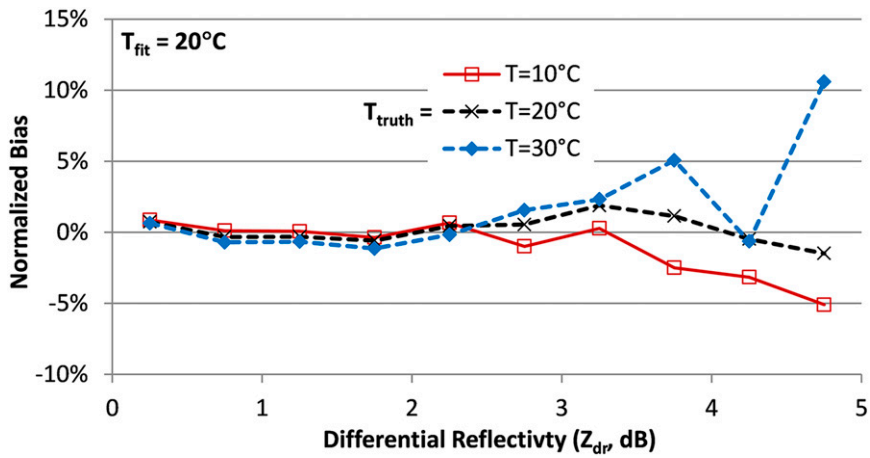

FIG. 13. Normalized bias (%) of the median volume diameter (D_0) estimated from the best-fit polynomial, $D_0(Z_{dr})_{fit}$, as a function of binned Z_{dr} assuming a drop temperature for the fit equation of T_{fit} = 20°C relative to a truth dataset with temperatures varying as shown by the colored lines in the figure key (i.e., T_{truth} = 10°C: solid red, T_{truth} = 20°C: dashed black, T_{truth} = 30°C: dashed blue). The maximum drop diameter was assumed to be $D_{max} = 3.5D_0$ for this temperature sensitivity test. The radar wavelength was C band. All other rain properties were as discussed in section 2a.

postulated $(D_{max})_{fit}$ and $(D_{max})_{truth}$. Normalized bias errors for $D_0(Z_{dr})_{fit}$ at C band ranged from −8% to 15%, again depending on the postulated error in D_{max} (Fig. 7). The magnitude of the potential bias error in the estimated D_0 from C-band Z_{dr} is larger than has been noted in a number of early studies at S band (i.e., 5%). Importantly, the absolute normalized bias error for $D_0(Z_{dr})_{fit}$ at C band increases with Z_{dr}, can reach 10% for Z_{dr} as low as 1–1.75 dB and can increase from there to values as large as 15%–45% for larger Z_{dr} when the mismatch between the assumed $(D_{max})_{fit}$ and $(D_{max})_{truth}$ is large (Fig. 9). For $Z_{dr} \geq 1.5$ dB, the magnitude of the potential bias error in the estimated D_0 is larger for C-band Z_{dr} than it is for S-band and X-band Z_{dr} (Fig. 11) because of resonance scattering effects in large drops >5 mm (Fig. 2). For $Z_{dr} < 1.5$ dB, the bias errors in D_0 retrievals for X-band Z_{dr} are larger than for C and S band because of resonant scattering at X band in smaller drops (e.g., 3–4 mm as seen in Fig. 2). As expected, the normalized scatter error is not as greatly affected by variability in the D_{max} assumption (Figs. 8 and 10) and is largely controlled by the assumed standard error in Z_{dr}. For a fairly large temperature mismatch of 10°C, the overall bias of $D_0(Z_{dr})_{fit}$ is negligible (≈0 dB) in the mean over the full range of Z_{dr} (i.e., for all DSDs). For larger Z_{dr} values, the $D_0(Z_{dr})_{fit}$ bias error can approach ±5%–10% for a temperature bias of ±10°C (Fig. 13). While these errors are not trivial, it is worthwhile to note that the impact of D_{max} uncertainty is likely often larger than the impact of temperature uncertainty on the accuracy of the $D_0(Z_{dr})_{fit}$ estimator (cf. Figs. 9 and 13).

As noted by others (e.g., Ulbrich 1992; Smith et al. 1993), estimating the appropriate maximum drop diameter of a DSD from a single disdrometer measurement over a period that is consistent with the spatial scale of radar data is difficult if not futile based on sampling limitations and may often underestimate D_{max}. On the other hand, using larger D_{max} (e.g., $\geq 2.5D_0$) for all DSD that are exceedingly rare (i.e., occurrence at 95th to 99th percentile or larger) in single disdrometer measurements consistent with radar resolution volume spatial scales could potentially overestimate D_{max}. As shown in this study, this uncertainty in D_{max} has implications for the estimated bias error in retrieved D_0 using Z_{dr}, especially at C band because of resonance.

Without reducing this uncertainty, D_{max} is currently a tunable parameter in the radar retrieval model that can be adjusted to maximize agreement between polarimetric radar and independently observed (e.g., disdrometers, wind profilers) estimates of D_0, assuming independent measurements of drop size are available. If adjustments to D_{max} are made to optimize agreement, then this uncertainty in D_{max} could be masking other potential sources of polarimetric radar bias error. Regardless of whether independent measurements of drop size are available or not, it would be highly desirable to reduce uncertainty in D_{max} associated with a given DSD to increase the robustness of the polarimetric radar estimate of D_0, especially at C band. Ongoing efforts to reduce uncertainty in D_{max} include dense networks of many disdrometers distributed within a typical radar footprint (e.g., Jaffrain and Berne 2012; Petersen et al.

2013). Including many disdrometers within a dense network will increase the instantaneous DSD sample size in a typical radar footprint and potentially reduce the uncertainty in estimating D_{max} relative to a single disdrometer, which is what has been typically done.

Until methods for estimating D_{max} and knowledge for parameterizing D_{max} improve, we recommend using the $D_{max} = 3D_0$ assumption as it minimizes the error relative to the possible upper range of C that is typically observed in disdrometer data and assumed in the literature, as can be seen in Fig. 7. We also strongly recommend that investigators note the uncertainty in their D_{max} parameterization and resulting impact on their results based on this study.

Future work will include detailed intercomparisons of very large samples of polarimetric radar and 2DVD disdrometer estimated D_0 values using both targeted NASA GPM Ground Validation (GV) field campaign (i.e., several weeks to several months with ancillary precipitation observations) and multiyear fixed site observational datasets such as the ARMOR C-band radar and the CSU 2DVD in Huntsville. In this way, methods for estimating D_0 from C-band radar will continue to be improved and uncertainty reduced.

Acknowledgments. This research is funded by Dr. Ramesh Kakar, NASA Precipitation Measurement Mission (PMM), Dr. Gail Skofronick-Jackson, NASA GPM Project Scientist, and Dr. Mathew Schwaller, NASA GPM Project Office under the following NASA Contracts: NNM05AA22A, NNM11AA01A, and NNX13AI89G. We also acknowledge the late Dr. Arthur Hou, whose leadership as the former NASA GPM Project Scientist was essential to the success of the GPM program and the realization of this study. We thank Patrick Gatlin, Matt Wingo, and Chris Schultz for their careful operation and maintenance of the 2DVD units at the NSSTC berm in Huntsville over many years. We thank Dr. V. N. Bringi for the use of the CSU 2DVD data, close collaboration, scientific leadership in the retrieval of raindrop characteristics from polarimetric radar, and his insight into this research. We acknowledge the many members of the NASA PMM DSD Working Group who have provided ideas, insightful comments, and encouragement during the conduct of this research, including Mr. Patrick Gatlin, Dr. Ali Tokay, Dr. Merhala Thurai, and Dr. Chris Williams. Constructive comments from four anonymous reviewers greatly improved the clarity of the text and figures.

REFERENCES

Andsager, K., K. V. Beard, and N. F. Laird, 1999: Laboratory measurements of axis ratios for large raindrops. *J. Atmos. Sci.,* **56,** 2673–2683, doi:10.1175/1520-0469(1999)056<2673:LMOARF>2.0.CO;2.

Aydin, K., and V. Giridhar, 1992: C-band dual-polarization radar observables in rain. *J. Atmos. Oceanic Technol.,* **9,** 383–390, doi:10.1175/1520-0426(1992)009<0383:CBDPRO>2.0.CO;2.

——, H. Direskeneli, and T. Seliga, 1987: Dual-polarization radar estimation of rainfall parameters compared with ground-based disdrometer measurements: October 29, 1982 central Illinois experiment. *IEEE Trans. Geosci. Remote Sens.,* **GE-25,** 834–844, doi:10.1109/TGRS.1987.289755.

Barber, P., and C. Yeh, 1975: Scattering of electromagnetic waves by arbitrary shaped dielectric bodies. *Appl. Opt.,* **14,** 2864–2872, doi:10.1364/AO.14.002864.

Beard, K. V., and C. Chuang, 1987: A new model for the equilibrium shape of raindrops. *J. Atmos. Sci.,* **44,** 1509–1524, doi:10.1175/1520-0469(1987)044<1509:ANMFTE>2.0.CO;2.

——, and R. J. Kubesh, 1991: Laboratory measurements of small raindrop distortion. Part II: Oscillation frequencies and modes. *J. Atmos. Sci.,* **48,** 2245–2264, doi:10.1175/1520-0469(1991)048<2245:LMOSRD>2.0.CO;2.

——, D. B. Johnson, and D. Baumgardner, 1986: Aircraft observations of large raindrops in warm, shallow, convective clouds. *Geophys. Res. Lett.,* **13,** 991–994, doi:10.1029/GL013i010p00991.

——, R. J. Kubesh, and H. T. Ochs, 1991: Laboratory measurements of small raindrop distortion. Part I: Axis ratios and fall behavior. *J. Atmos. Sci.,* **48,** 698–710, doi:10.1175/1520-0469(1991)048<0698:LMOSRD>2.0.CO;2.

Brandes, E. A., G. Zhang, and J. Vivekanandan, 2002: Experiments in rainfall estimation with a polarimetric radar in a subtropical environment. *J. Appl. Meteor.,* **41,** 674–685, doi:10.1175/1520-0450(2002)041<0674:EIREWA>2.0.CO;2, Corrigendum, **44,** 186, doi:10.1175/1520-0450(2005)44<186:C>2.0.CO;2.

——, ——, and ——, 2003: An evaluation of a drop distribution-based polarimetric radar rainfall estimator. *J. Appl. Meteor.,* **42,** 652–660, doi:10.1175/1520-0450(2003)042<0652:AEOADD>2.0.CO;2.

——, ——, and ——, 2004a: Comparison of polarimetric radar drop size distribution retrieval algorithms. *J. Atmos. Oceanic Technol.,* **21,** 584–598, doi:10.1175/1520-0426(2004)021<0584:COPRDS>2.0.CO;2.

——, ——, and ——, 2004b: Drop size distribution retrieval with polarimetric radar: Model and application. *J. Appl. Meteor.,* **43,** 461–475, doi:10.1175/1520-0450(2004)043<0461:DSDRWP>2.0.CO;2.

Bringi, V. N., and V. Chandrasekar, 2001: *Polarimetric Doppler Weather Radar: Principles and Applications.* Cambridge University Press, 636 pp.

——, ——, P. Meischner, J. Hubbert, and Y. Golestani, 1991: Polarimetric radar signatures of precipitation at S- and C-bands. *IEE Proc. F Radar Signal Process.,* **138,** 109–119.

——, ——, and R. Xiao, 1998: Raindrop axis ratios and size distributions in Florida rainshafts: An assessment of multiparameter radar algorithms. *IEEE Trans. Geosci. Remote Sens.,* **36,** 703–715, doi:10.1109/36.673663.

——, G.-J. Huang, and V. Chandrasekar, 2002: A methodology for estimating the parameters of a gamma raindrop size distribution model from polarimetric radar data: Application to a squall-line event from the TRMM/Brazil Campaign. *J. Atmos. Oceanic Technol.,* **19,** 633–645, doi:10.1175/1520-0426(2002)019<0633:AMFETP>2.0.CO;2.

——, V. Chandrasekar, J. Hubbert, E. Gorgucci, W. L. Randeu, and M. Schoenhuber, 2003: Raindrop size distribution in different climatic regimes from disdrometer and dual-polarized

radar analysis. *J. Atmos. Sci.,* **60,** 354–365, doi:10.1175/1520-0469(2003)060<0354:RSDIDC>2.0.CO;2.

——, M. Thurai, K. Nakagawa, G. J. Huang, T. Kobayashi, A. Adachi, H. Hanado, and S. Sekizawa, 2006: Rainfall estimation from C-band polarimetric radar in Okinawa, Japan: Comparisons with 2D-video disdrometer and 400 MHz wind profiler. *J. Meteor. Soc. Japan,* **84,** 705–724, doi:10.2151/jmsj.84.705.

——, C. R. Williams, M. Thurai, and P. T. May, 2009: Using dual-polarized radar and dual-frequency profiler for DSD characterization: A case study from Darwin, Australia. *J. Atmos. Oceanic Technol.,* **26,** 2107–2122, doi:10.1175/2009JTECHA1258.1.

Cao, Q., and G. Zhang, 2009: Errors in estimating raindrop size distribution parameters employing disdrometer and simulated raindrop spectra. *J. Appl. Meteor. Climatol.,* **48,** 406–425, doi:10.1175/2008JAMC2026.1.

——, ——, E. Brandes, T. Schuur, A. Ryzhkov, and K. Ikeda, 2008: Analysis of video disdrometer and polarimetric radar data to characterize rain microphysics in Oklahoma. *J. Appl. Meteor. Climatol.,* **47,** 2238–2255, doi:10.1175/2008JAMC1732.1.

Carey, L. D., S. A. Rutledge, D. A. Ahijevych, and T. D. Keenan, 2000: Correcting propagation effects in C-band polarimetric radar observations of tropical convection using differential propagation phase. *J. Appl. Meteor.,* **39,** 1405–1433, doi:10.1175/1520-0450(2000)039<1405:CPEICB>2.0.CO;2.

Chandrasekar, V., W. A. Cooper, and V. N. Bringi, 1988: Axis ratios and oscillations of raindrops. *J. Atmos. Sci.,* **45,** 1323–1333, doi:10.1175/1520-0469(1988)045<1323:ARAOOR>2.0.CO;2.

——, A. Hou, E. Smith, V. N. Bringi, S. A. Rutledge, E. Gorgucci, W. A. Petersen, and G. Skofronick Jackson, 2008: Potential role of dual-polarization radar in the validation of satellite precipitation measurements: Rationale and opportunities. *Bull. Amer. Meteor. Soc.,* **89,** 1127–1145, doi:10.1175/2008BAMS2177.1.

Fujiyoshi, Y., I. Yamamura, N. Nagumo, K. Nakagawa, K. Muramoto, and T. Shimomai, 2008: The maximum size of raindrops—Can it be a proxy of precipitation climatology? *Extended Abstracts, Int. Conf. on Clouds and Precipitation,* Cancun, Mexico, International Commission on Clouds and Precipitation, P1.31. [Available online at http://cabernet.atmosfcu.unam.mx/ICCP-2008/abstracts/Program_on_line/Poster_01/Fujiyoshi_extended.pdf.]

Gatlin, P. N., M. Thurai, V. N. Bringi, W. Petersen, D. Wolff, A. Tokay, L. Carey, and M. Wingo, 2015: Searching for large raindrops: A global summary of two-dimensional video disdrometer observations. *J. Appl. Meteor. Climatol.,* **54,** 1069–1089, doi:10.1175/JAMC-D-14-0089.1.

Goddard, J. W. F., and S. M. Cherry, 1984: The ability of dual-polarization radar (copolar linear) to predict rainfall rate and microwave attenuation. *Radio Sci.,* **19,** 201–208, doi:10.1029/RS019i001p00201.

——, ——, and V. N. Bringi, 1982: Comparison of dual-polarization radar measurements of rain with ground-based disdrometer measurements. *J. Appl. Meteor.,* **21,** 252–256, doi:10.1175/1520-0450(1982)021<0252:CODPRM>2.0.CO;2.

——, J. D. Eastment, and J. Tan, 1994: Self-consistent measurements of differential phase and differential reflectivity in rain. *Proc. 1994 Int. Geoscience and Remote Sensing Symp.*, Pasadena, CA, IEEE, 369–371.

Gorgucci, E., G. Scarchilli, and V. Chandrasekar, 1999: A procedure to calibrate multiparameter weather radar using properties of the rain medium. *IEEE Trans. Geosci. Remote Sens.,* **37,** 269–276, doi:10.1109/36.739161.

——, V. Chandrasekar, V. N. Bringi, and G. Scarchilli, 2002: Estimation of raindrop size distribution parameters from polarimetric radar measurements. *J. Atmos. Sci.,* **59,** 2373–2384, doi:10.1175/1520-0469(2002)059<2373:EORSDP>2.0.CO;2.

Hobbs, P. V., and A. L. Rangno, 2004: Super-large raindrops. *Geophys. Res. Lett.,* **31,** L13102, doi:10.1029/2004GL020167.

Hou, A. Y., and Coauthors, 2014: The Global Precipitation Measurement (GPM) Mission. *Bull. Amer. Meteor. Soc.,* **95,** 701–722, doi:10.1175/BAMS-D-13-00164.1.

Huang, G.-J., V. N. Bringi, and M. Thurai, 2008: Orientation angle distributions of drops after an 80-m fall using a 2D video disdrometer. *J. Atmos. Oceanic Technol.,* **25,** 1717–1723, doi:10.1175/2008JTECHA1075.1.

Jaffrain, J., and A. Berne, 2012: Quantification of the small-scale spatial structure of the raindrop size distribution from a network of disdrometers. *J. Appl. Meteor. Climatol.,* **51,** 941–953, doi:10.1175/JAMC-D-11-0136.1.

Jameson, A. R., 1983: Microphysical interpretation of multi-parameter radar measurements in rain. Part I: Interpretation of polarization measurements and estimation of raindrop shapes. *J. Atmos. Sci.,* **40,** 1792–1802, doi:10.1175/1520-0469(1983)040<1792:MIOMPR>2.0.CO;2.

——, 1994: An alternative approach to estimating rainfall rate by radar using propagation differential phase shift. *J. Atmos. Oceanic Technol.,* **11,** 122–131, doi:10.1175/1520-0426(1994)011<0122:AAATER>2.0.CO;2.

Kamra, A. K., R. V. Bhalwankar, and A. B. Sathe, 1991: Spontaneous breakup of charged and uncharged water drops freely suspended in a wind tunnel. *J. Geophys. Res.,* **96,** 17 159–17 168, doi:10.1029/91JD01475.

Keenan, T. D., L. D. Carey, D. S. Zrnić, and P. T. May, 2001: Sensitivity of 5-cm wavelength polarimetric radar variables to raindrop axial ratio and drop size distribution. *J. Appl. Meteor.,* **40,** 526–545, doi:10.1175/1520-0450(2001)040<0526:SOCWPR>2.0.CO;2.

Levenberg, K., 1944: A method for the solution of certain nonlinear problems in least squares. *Quart. J. Appl. Math.,* **2,** 164–168.

Marquardt, D., 1963: An algorithm for least-squares estimation of nonlinear parameters. *SIAM J. Appl. Math.,* **11,** 431–441, doi:10.1137/0111030.

Meischner, P. F., V. N. Bringi, D. Heimann, and H. Höller, 1991: A squall line in southern Germany: Kinematics and precipitation formation as deduced by advanced polarimetric and Doppler radar measurements. *Mon. Wea. Rev.,* **119,** 678–701, doi:10.1175/1520-0493(1991)119<0678:ASLISG>2.0.CO;2.

Petersen, W. A., and Coauthors, 2005: The UAH-NSSTC/WHNT ARMOR C-band dual-polarimetric radar: A unique collaboration in research, education and technology transfer. *Extended Abstracts, 32nd Conf. on Radar Meteorology,* Albuquerque, NM, Amer. Meteor. Soc., 12R.4. [Available online at https://ams.confex.com/ams/pdfpapers/96524.pdf.]

——, K. R. Knupp, D. J. Cecil, J. R. Mecikalski, C. Darden, and J. Burks, 2007: The University of Alabama Huntsville THOR center instrumentation: Research and operational collaboration. *Extended Abstracts, 33rd Int. Conf. on Radar Meteorology,* Cairns, Australia, Amer. Meteor. Soc., 5.1. [Available online at https://ams.confex.com/ams/pdfpapers/123410.pdf.]

——, V. N. Bringi, V. Chandrasekar, S. A. Rutledge, D. B. Wolff, A. Tokay, L. D. Carey, and M. Thurai, 2013: Radar deployments and field sampling for GPM ground validation field campaigns. *Proc. 36th Conf. on Radar Meteorology,* Breckenridge, CO, Amer. Meteor. Soc., 179. [Available online at https://ams.confex.com/ams/36Radar/webprogram/Handout/Paper228660/Petersen_etal_RadConf2013_Poster.pdf.]

Rauber, R. M., K. V. Beard, and B. M. Andrews, 1991: A mechanism for giant raindrop formation in warm, shallow convective clouds. *J. Atmos. Sci.,* **48,** 1791–1797, doi:10.1175/1520-0469(1991)048<1791:AMFGRF>2.0.CO;2.

Ryzhkov, A., and D. Zrnić, 2005: Radar polarimetry at S, C, and X bands: Comparative analysis and operational implications. *Extended Abstracts, 32nd Conf. on Radar Meteorology,* Albuquerque, NM, Amer. Meteor. Soc., 9R.3. [Available online at https://ams.confex.com/ams/pdfpapers/95684.pdf.]

Schönhuber, M., G. Lammer, and W. L. Randeu, 2008: The 2D-video-disdrometer. *Precipitation: Advances in Measurement, Estimation and Prediction,* S. Michaelides, Ed., Springer, 3–31.

Schuur, T. J., A. Ryzhkov, D. S. Zrnić, and M. Schönhuber, 2001: Drop size distributions measured by a 2D video disdrometer: Comparison with dual-polarization radar data. *J. Appl. Meteor.,* **40,** 1019–1034, doi:10.1175/1520-0450(2001)040<1019:DSDMBA>2.0.CO;2.

Seliga, T. A., and V. N. Bringi, 1976: Potential use of radar differential reflectivity measurements at orthogonal polarizations for measuring precipitation. *J. Appl. Meteor.,* **15,** 69–76, doi:10.1175/1520-0450(1976)015<0069:PUORDR>2.0.CO;2.

——, K. Aydin, and H. Direskeneli, 1986: Disdrometer measurements during an intense rainfall event in central Illinois: Implications for differential reflectivity radar observations. *J. Climate Appl. Meteor.,* **25,** 835–846, doi:10.1175/1520-0450(1986)025<0835:DMDAIR>2.0.CO;2.

Smith, P. L., Z. Liu, and J. Joss, 1993: A study of sampling-variability effects in raindrop size distributions. *J. Appl. Meteor.,* **32,** 1259–1269, doi:10.1175/1520-0450(1993)032<1259:ASOSVE>2.0.CO;2.

Tabary, P., G. Vulpiani, J. J. Gourley, A. J. Illingworth, R. J. Thompson, and O. Bousquet, 2009: Unusually high differential attenuation at C-band: Results from a two-year analysis of the French Trappes polarimetric radar data. *J. Appl. Meteor. Climatol.,* **48,** 2037–2053, doi:10.1175/2009JAMC2039.1.

Takahashi, T., K. Suzuki, M. Orita, M. Tokuno, and R. de la Mar, 1995: Videosonde observations of precipitation processes in equatorial cloud clusters. *J. Meteor. Soc. Japan,* **73,** 509–534.

Thurai, M., and V. N. Bringi, 2005: Drop axis ratios from 2D video disdrometer. *J. Atmos. Oceanic Technol.,* **22,** 966–978, doi:10.1175/JTECH1767.1.

——, G. J. Huang, V. N. Bringi, W. L. Randeu, and M. Schönhuber, 2007: Drop shapes, model comparisons, and calculations of polarimetric radar parameters in rain. *J. Atmos. Oceanic Technol.,* **24,** 1019–1032, doi:10.1175/JTECH2051.1.

——, M. Szakáll, V. N. Bringi, K. V. Beard, S. K. Mitra, and S. Borrmann, 2009: Drop shapes and axis ratio distributions: Comparison between 2D video disdrometer and wind-tunnel measurements. *J. Atmos. Oceanic Technol.,* **26,** 1427–1432, doi:10.1175/2009JTECHA1244.1.

——, W. A. Petersen, A. Tokay, C. Schultz, and P. Gatlin, 2011: Drop size distribution comparisons between Parsivel and 2-D video disdrometers. *Adv. Geosci.,* **30,** 3–9, doi:10.5194/adgeo-30-3-2011.

Ulbrich, C. W., 1983: Natural variations in the analytical form of the raindrop size distribution. *J. Climate Appl. Meteor.,* **22,** 1764–1775, doi:10.1175/1520-0450(1983)022<1764:NVITAF>2.0.CO;2.

——, 1985: The effects of drop size distribution truncation on rainfall integral parameters and empirical relations. *J. Climate Appl. Meteor.,* **24,** 580–590, doi:10.1175/1520-0450(1985)024<0580:TEODSD>2.0.CO;2.

——, 1992: Effects of drop-size-distribution truncation on computer simulations of dual-measurement radar methods. *J. Appl. Meteor.,* **31,** 689–699, doi:10.1175/1520-0450(1992)031<0689:EODSDT>2.0.CO;2.

——, and D. Atlas, 1984: Assessment of the contribution of differential polarization to improved rainfall measurements. *Radio Sci.,* **19,** 49–57, doi:10.1029/RS019i001p00049.

——, and ——, 1998: Rainfall microphysics and radar properties: Analysis methods for drop size spectra. *J. Appl. Meteor.,* **37,** 912–923, doi:10.1175/1520-0450(1998)037<0912:RMARPA>2.0.CO;2.

Vivekanandan, J., W. M. Adams, and V. N. Bringi, 1991: Rigorous approach to polarimetric radar modeling of hydrometeor orientation distributions. *J. Appl. Meteor.,* **30,** 1053–1063, doi:10.1175/1520-0450(1991)030<1053:RATPRM>2.0.CO;2.

Waterman, P. C., 1969: Scattering by dielectric obstacles. *Alta Freq.,* **38** (Speciale), 348–352.

Zhang, G., J. Vivekanandan, and E. Brandes, 2001: A method for estimating rain rate and drop size distribution from polarimetric radar measurements. *IEEE Trans. Geosci. Remote Sens.,* **39,** 830–841, doi:10.1109/36.917906.

Zrnić, D. S., T. D. Keenan, L. D. Carey, and P. May, 2000: Sensitivity analysis of polarimetric variables at a 5-cm wavelength in rain. *J. Appl. Meteor.,* **39,** 1514–1526, doi:10.1175/1520-0450(2000)039<1514:SAOPVA>2.0.CO;2.